BNL-104265-2014-JA

AGU PUBLICATIONS

JGR

Journal of Geophysical Research: Atmospheres

RESEARCH ARTICLE
10.1002/2013JD020841

Key Points:
- Sub-3 nm particles are not present all the time at Kent and Brookhaven
- Sub-3 nm particles were associated with sulfuric acid during the day
- There were nighttime sub-3 nm particles in the marine air masses at Brookhaven

Correspondence to:
Shan-Hu Lee,
slee19@kent.edu

Citation:
Yu, H., et al. (2014), Sub-3 nm particles observed at the coastal and continental sites in the United States, *J. Geophys. Res. Atmos.*, *119*, 860–879, doi:10.1002/2013JD020841.

Received 13 SEP 2013
Accepted 15 DEC 2013
Accepted article online 19 DEC 2013
Published online 27 JAN 2014

Sub-3 nm particles observed at the coastal and continental sites in the United States

Huan Yu[1,2], A. Gannet Hallar[3], Yi You[4], Arthur Sedlacek[5], Stephen Springston[5], Vijay P. Kanawade[2,6], Yin-Nan Lee[5], Jian Wang[5], Chongai Kuang[5], Robert L. McGraw[5], Ian McCubbin[3], Jyri Mikkila[7], and Shan-Hu Lee[2]

[1]Jiangsu Key Laboratory of Atmospheric Environment Monitoring and Pollution Control, School of Environmental Science and Engineering, Nanjing University of Information Science and Technology, Nanjing, China, [2]College of Public Health, Kent State University, Kent, Ohio, USA, [3]Storm Peak Laboratory, Division of Atmospheric Science, Desert Research Institute, Steamboat Springs, Colorado, USA, [4]Department of Chemistry, Kent State University, Kent, Ohio, USA, [5]Atmospheric Sciences Division, Brookhaven National Laboratory, Upton, New York, USA, [6]Department of Civil Engineering, Indian Institute of Technology, Kanpur, India, [7]Airmodus Oy, Helsinki, Finland

Abstract Direct measurements of atmospheric sub-3 nm particles are crucial for understanding the new particle formation mechanisms, but such measurements are very limited at present. We report measurements of sub-3nm particles at Brookhaven, New York (a coastal site in summer) and Kent, Ohio (a continental site in winter). During daytime, in approximately 80% of the observation days at both sites, sub-3nm particle events were observed with concentrations of 2800 ± 1600 cm^{-3}, and they appeared with the elevated sulfuric acid concentrations. During the nighttime at the coastal site under the marine air mass influences, there were also substantial concentrations of sub-3nm particles (1500 ± 400 cm^{-3}), but they did not grow larger. On the other hand, at the coastal Brookhaven site under the continental air mass influences and at the inland Kent site during the night, the sub-3nm particles were significantly lower (190 ± 130 cm^{-3}). Our results indicate that sub-3nm particles were not always present, and their presence was rather closely associated with specific aerosol nucleation precursors: sulfuric acid and other unknown condensable chemical species likely present in the marine air masses. These findings are thus different from other studies conducted in the Finland boreal forest, which showed a persistent presence of high concentrations of sub-2nm particles and that these sub-2nm particles were more correlated to monoterpene oxidation products than to sulfuric acid. Therefore, different nucleation mechanisms, as opposed on to a universal mechanism, involving different nucleation precursors dominate in different atmospheric environments with different emissions and transported trace gases.

1. Introduction

New particle formation (NPF) is an important source of secondary aerosols in the atmosphere [*Seinfeld and Pandis*, 2006] and contributes significantly to the global production of cloud condensation nuclei (CCN) [*Merikanto et al.*, 2009]. NPF consists of two steps: formation of molecular clusters from gas phase species (nucleation) and growth of these clusters to aerosol particles [*Kulmala et al.*, 2004b; *Zhang et al.*, 2012]. CCN production rates and the impact of anthropogenic and natural emissions on these rates are crucial for quantifying the aerosol indirect effects on the radiative forcing of climate. There are currently several nucleation mechanisms, including sulfuric acid–water (H_2SO_4–H_2O) binary homogeneous nucleation [*Ball et al.*, 1999; *Benson et al.*, 2008; *Berndt et al.*, 2005; *Sipila et al.*, 2010; *Vehkamäki et al.*, 2002; *Wyslouzil et al.*, 1991; *Young et al.*, 2008], sulfuric acid-water-ammonia (H_2SO_4–H_2O–NH_3) ternary homogeneous nucleation [*Benson et al.*, 2009, 2011; *Berndt et al.*, 2010; *Kirkby et al.*, 2011; *Korhonen et al.*, 1999; *Weber et al.*, 1996], multicomponent nucleation involving organic compounds [*Berndt et al.*, 2010; *Chen et al.*, 2012; *Dawson et al.*, 2012; *Erupe et al.*, 2011; *Metzger et al.*, 2010; *O'Dowd et al.*, 2002a, 2002b; *Riccobono et al.*, 2012; *Zhang et al.*, 2004; *Zollner et al.*, 2012], and ion-induced nucleation [*Laakso et al.*, 2004; *Lee et al.*, 2003; *Lovejoy et al.*, 2004; *Yu et al.*, 1998]. For the growth of nucleated clusters, various organic compounds may play important roles [*Donahue et al.*, 2011; *Riipinen et al.*, 2012; *Wang and Wexler*, 2013]. Aerosol nucleation and growth processes are not well understood, largely due to the limited measurements of aerosol nucleation precursors (H_2SO_4, NH_3, amines, and organic acids), aerosol sizes and

concentrations of newly formed sub-3 nm particles, and chemical composition of nucleation clusters under a variety of atmospheric conditions.

Recently, a series of new instruments have been developed to detect aerosol chemical composition and number concentrations of sub-3 nm particles, such as cluster-CIMS (chemical ionization mass spectrometer) [*Zhao et al*., 2010], Atmospheric Pressure interface Time-Of-Flight mass spectrometer (APi-TOF) [*Junninen et al*., 2010], Chemical Ionization Atmospheric Pressure interface Time-Of-Flight mass spectrometer (CI-APi-TOF) [*Jokinen et al*., 2012], natural air ion spectrometer (NAIS) [*Kulmala et al*., 2007], diethylene glycol scanning mobility particle spectrometer (DEG)-(SMPS) [*Jiang et al*., 2011a], particle size magnifier (PSM) [*Vanhanen et al*., 2011], pulse-height condensation particle counter (PH-CPC) [*Sipila et al*., 2009], and symmetric inclined grid mobility analyzer [*Tammet*, 2011]. Based on the sub-3 nm particle concentrations and sizes measured with NAIS, PSM, and PH-CPC in the Hyytiälä boreal forest [*Kulmala et al*., 2007, 2013; *Lehtipalo et al*., 2009, 2010, 2011], Kulmala and colleagues have concluded that there were always a pool of sub-2 nm neutral clusters during the day and night, but they may be not important for NPF and rather the activation of these small clusters by H_2SO_4, NH_3, amines, and organic acids play key roles for the growth of these clusters to aerosol particles [*Kulmala et al*., 2013]. This proposed nanoactivation process is similar to Kohler's cloud droplet activation theory [*Kulmala et al*., 2004a], except that this process occurs on nanometer size particles, initiated by specific chemical compounds. However, it is unclear what are the chemical mechanisms behind this nanoactivation process, and if the persistent presence of sub-2 nm particles is unique to the Hyytiälä boreal forest (with high emissions of monoterpenes over isoprene) and whether such activation parameterization can be applicable to other regions of the Earth's atmosphere [*Andreae*, 2013]. For example, measurements with PH-CPC at the Mace Head in Ireland, on the other hand, indicated that concentrations of sub-3 nm particles were much lower than those observed in the Hyytiälä forest, in general, and at this coast site, NPF may take place via homogeneous nucleation processes as opposed to the nanoactivation process [*Lehtipalo et al*., 2010]. McMurry and colleagues made measurements of neutral cluster measurements with the cluster-CIMS and DEG-SMPS under high-sulfur plume conditions (in Boulder, Colorado and Atlanta, Georgia) and reported clusters containing four molecules of H_2SO_4 [*Chen et al*., 2012; *Jiang et al*., 2011b; *Zhao et al*., 2010, 2011]. Based on these observations, they proposed that the formation of clusters containing two H_2SO_4 and some base molecules may be the bottleneck in aerosol nucleation processes [*Chen et al*., 2012].

Most of NPF observations have been made during the daytime when photochemical processes with UV lights (and hence the photochemical production of OH and H_2SO_4) are active, and studies of nighttime NPF are very limited. Regardless, there are several observations that have shown nighttime particle formation events in various atmospheric conditions [*Junninen et al*., 2008; *Lehtipalo et al*., 2011; *Ortega et al*., 2009, 2012; *Russell et al*., 2007; *Suni et al*., 2008; *Svenningsson et al*., 2008; *Wiedensohler et al*., 1997], even in the free troposphere [*Hermann et al*., 2003; *Lee et al*., 2008], but the mechanisms behind the nighttime nucleation are yet still highly speculative. It is possible that some heterogeneous oxidation processes can produce dark oxidants, in a similar manner as on the wet surfaces of cloud and fog droplets via catalytic reactions by transition metals [*Finlayson-Pitts and Pitts*, 2000; *Harris et al*., 2013; *Seinfeld and Pandis*, 2006], to contribute to NPF during the nighttime [*Lee et al*., 2008]. It is also possible that biogenic volatile organic compounds (VOCs) can react with ozone to produce particles even in the absence of UV light [*Hoffmann et al*., 1997; *Ortega et al*., 2012]. Additionally, OH can be produced from ozone and VOCs reactions [*Donahue et al*., 1998; *Paulson et al*., 1999, 1997], which in turn react with SO_2 to produce H_2SO_4 and new particles. *Mauldin et al.* [2012] recently suggested that stabilized *Criegee* intermediate oxidants, produced from the biogenic volatile organic compounds (VOCs) ozonolysis reactions, can directly interact with SO_2 to produce H_2SO_4, but it is unclear whether such stabilized Criegee intermediate processes also contribute to the nighttime NPF.

In the present study, we report measurements of sub-3 nm particles and H_2SO_4 concentrations made at two distinctive sites in the United States: Brookhaven, New York (a costal site with influences of either marine or continental air masses), and Kent, Ohio (an inland continental site affected by frequent sulfur plumes). From these measurements, we examined whether sub-3 nm particles were always present (Kent versus Brookhaven; day versus night) and how chemical species were correlated to the formation of sub-3 nm particles (marine air mass versus continental air mass). To our knowledge, this is the first time that PSM measurements of 3 nm particles are reported from Northern American sites.

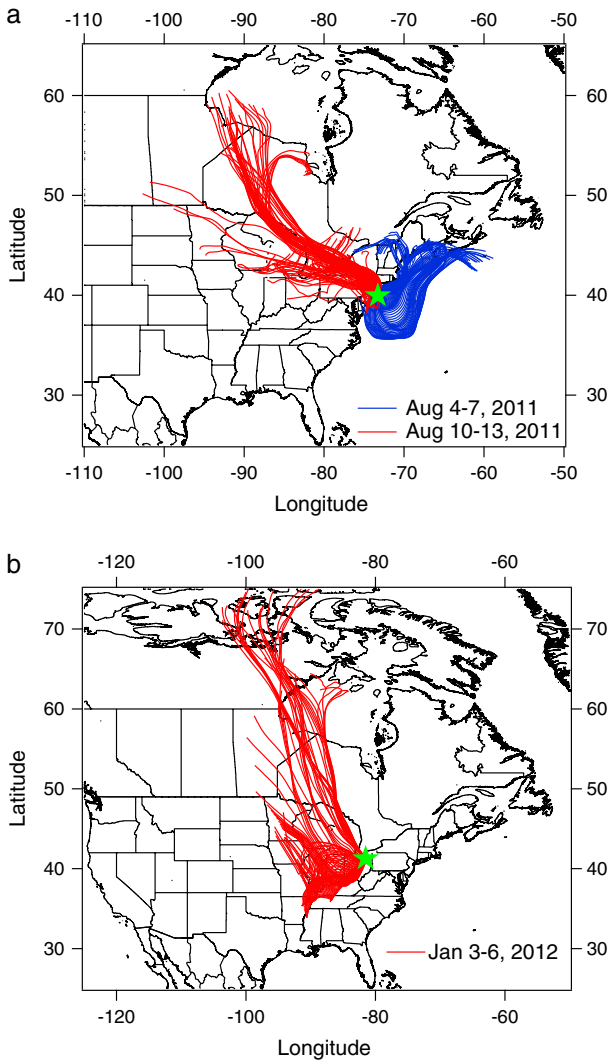

Figure 1. Three day back trajectories arriving at (a) Brookhaven, New York, and (b) Kent, Ohio, for the chosen days, calculated hourly from NOAA HYSPLIT. The two sampling sites are shown as green stars. During 10–13 August 2011 (red trajectories) the Brookhaven site was characterized by continental air masses with distinctive banana-shaped NPF events. On 4–7 August 2011(blue trajectories) this site was characterized by marine air mass and clear nighttime events. The Kent site had NPF events from 3 to 6 January 2012 (red trajectories).

2. Experiments

We report the measurements conducted at two sites: Brookhaven, New York, and Kent, Ohio. The first measurement was made at Brookhaven National Laboratory in Long Island, New York (40.871°N, 72.89°W, 24 m above sea level; indicated by a green star in Figure 1a), during the 2011 Department of Energy Aerosol Life Cycle Intense Observation Period (IOP) study [*Sedlacek et al.*, 2012]. New York City is located 80 km west of this site (Brookhaven for short hereafter). The Atlantic Ocean is 25 km to the south-southeast and Long Island Sound (an estuary of the Atlantic Ocean) is 16 km to the north. This site is characterized by a small urban township and surrounded by a mixed forest that consists of various pine and oak trees. Continuous measurements of particle and key trace gas phase species including H_2SO_4 were made for 23 days between 22 July and 13 August 2011.

Total number concentrations of particles down to 1 nm diameter were measured with a particle size magnifier (PSM, AirModus A09) using diethylene glycol (DEG) as working fluid at a flow rate of 1 standard litter per minute (slpm) [*Vanhanen et al.*, 2011]. The working principle of PSM is to mix the turbulently cooled sample flow with a heated clean airflow saturated by the DEG fluid. This creates high saturation ratios of the working fluid to activate the seed particles and grow them by condensation. A PSM can grow particles as small as 1 nm to larger

than 90 nm, after which a CPC is used to count the grown particles. Two types of nanoparticles were used for calibration at room temperature by AirModus: the mobility standards (tetraalkyl ammonium halides) produced by electrospray from methanol solution and silver particles produced in a tube furnace and charged with a bipolar Am-241 charger. The detection efficiencies of these nanoparticles are ~100% (3 nm), ~89% (2 nm), and ~40% (1 nm), respectively, at a DEG flow rate of 1 slpm. In comparison, at a flow rate of 0.2 slpm of the DEG saturator fluid, the detection efficiencies are ~95% (3 nm), 56% (2 nm), and 0% (1 nm), respectively. The composition and charge of atmospheric particles are different from the laboratory-generated particles, and this can affect the activation efficiency of particles in the PSM. Based on the laboratory calibration, it was estimated that the unknown composition and charge of the atmospheric particles can lead to an error of about 0.2 nm in the size determination of the particles, and an error of tens of percent (in absolute units) in the detection efficiency [*Kulmala et al*., 2013]. We defined the detection limit of PSM as 3 times the standard deviation of background signals, which were obtained by adding a high-efficiency particulate absorption (HEPA) filter before the PSM inlet to remove particles. PSM detection limits were determined to be 40 cm^{-3} and 24 cm^{-3} at 1.0 slpm and 0.2 slpm saturator flow rates, respectively.

We measured the total number concentrations of particles larger than 1 nm with PSM using a constant fluid flow rate of 1.0 slpm. We did not scan the PSM fluid flow rates between 0.1 and 1.0 slpm, and the exact detection efficiency curves at all these flow rates were unknown, so we did not invert particle sizes below 3 nm. We define here N_{tot} as the total particle concentration measured by PSM at 1.0 slpm with a 1.3 nm cutoff size (D_{50}, where 50% particles are detected). If the median diameter of a nucleation mode is close to 3 nm, N_{tot} would represent ~100% of total particle number. On another extreme, when a nucleation mode is around 1 nm, N_{tot} would account for 40% of total particles. When assuming a lognormal mode of 2 nm median diameter and 1.2 standard deviation, N_{tot} would account for 83% of the total particle number concentration. Therefore, the magnitude or diurnal variation of sub-3 nm particle concentrations was unlikely changed by using N_{tot}, because we have observed sub-3 nm particles in the events were 1 order of magnitude higher than those during the nonevent periods (as will be discussed in detail in section 3).

It is also possible that the detection efficiency of small particles in the PSM is suppressed in the presence of large particles, because the DEG working fluid can be preferably condensed on large particles than on small particles below 3 nm. To examine this issue, we generated newly nucleated H_2SO_4 particles in the size of ~1.3 nm with a particle number concentration of 6.2×10^3 cm^{-3} in a fast flow nucleation tube at [H_2SO_4] of 7×10^6 cm^{-3} via homogeneous nucleation (following the experimental procedure described by [*Yu et al*., 2012]). Before entering the PSM (inlet flow rate: 2.5 slpm), the flow of newly formed particles was diluted by another flow 0.5–2.0 slpm containing $(NH_4)_2SO_4$ particles. The $(NH_4)_2SO_4$ particles, which were generated from a Trust, Science, and Innovation (TSI) 9302 atomizer (TSI, Inc., St. Paul, MN, U.S.A.) and a diffusion dryer, had a mode diameter of 160 nm diameter and a concentration of 10^4 cm^{-3} in the diluting flow. After subtracting the $(NH_4)_2SO_4$ particle number concentration, the H_2SO_4 particles were measured to be 5900–6300 cm^{-3}, accounting for 95–102% of the particle concentration in the flow tube. This indicates that the DEG vapor depletion due to large aerosol particles did not occur under typical measurement conditions.

Both neutral and charged particles can be activated in PSM, thus PSM cannot distinguish the neutral versus charged clusters and particles. However, it is a general understanding in the field that charged particles only represent a very small fraction of the total particles in the typical lower tropospheric conditions [*Eisele et al*., 2006; *Hirsikko et al*., 2011; *Kulmala et al*., 2013; *Lovejoy et al*., 2004], although there is also an argument that ion recombination can be important for the formation of neutral clusters [*Yu et al*., 2008]. We thus assumed that the sub-3 nm particles measured with PSM were mostly composed of neutral clusters and particles at these two ground sites.

Particle number concentrations in the size range from 3 to 478 nm (N_{3-478}) and their size distributions were obtained by integrating two scanning mobility particle spectrometer (SMPS) measurements with a nano-SMPS (a TSI differential mobility analyzer DMA3085 and a condensation particle counter CPC3776, measuring particles in the size range from 3 to 64 nm) and a long-SMPS (TSI DMA3081 and CPC3772, from 10 to 478 nm). We performed a correlation analysis on the total particle concentrations in the overlapped size range between 10 and 64 nm measured by the two SMPS systems (nano-SMPS versus long-SMPS). The correlation coefficient (R^2) of 0.94 with a slope of 1.03 indicated a good agreement between the two SMPSs. N_{3-478} were thus calculated from the sum of the N_{3-64} obtained from the nano-SMPS and the N_{64-478} from the long-SMPS.

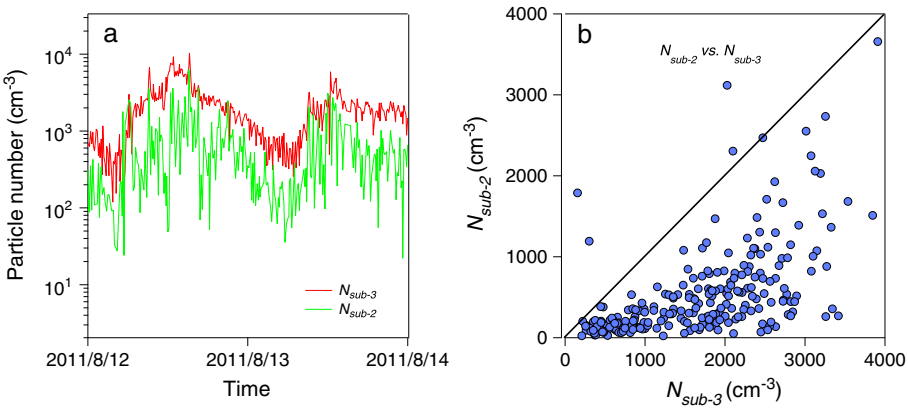

Figure 2. Sub-3 nm particle concentration ($N_{sub\text{-}3}$) and sub-2 nm particle concentration ($N_{sub\text{-}2}$) during 12–14 August 2011 at Brookhaven, NY. (a) Time series of $N_{sub\text{-}3}$ and $N_{sub\text{-}2}$ and (b) $N_{sub\text{-}2}$ versus $N_{sub\text{-}3}$.

We also assumed that $N_{3–478}$ were nearly the same as the total number concentrations of particles larger than 3 nm, since coarse mode particles usually represent only a very small fraction of the total aerosol number concentrations. Then, the difference between N_{tot} and $N_{3–478}$ corresponded to the total sub-3 nm particle concentration measured by PSM between 1.3 nm (D_{50} of PSM at 1.0 slpm) and 3 nm, not accounting for the transport loss in the sampling line. During the measurement, a 2.1 m long and 5.08 cm diameter tube drew the ambient air into the instrument container with a sampling flow rate of 150 slpm. PSM then sampled from a split flow of 30 slpm in a 30 cm long and 2.54 cm diameter tube. The transport loss in front of the PSM was estimated to be 10% and 35% for 3 nm to 1 nm particles, respectively. Because the exact size distribution in the 1–3 nm size range was unknown, $N_{sub\text{-}3}$ was obtained by correcting with an average transport loss of 22%.

For some short periods of the IOP study (30 July to 1 August; 7–8 August), SMPS data measurements were not available, so particles in the size smaller than 2 nm ($N_{sub\text{-}2}$) were used instead of $N_{sub\text{-}3}$ for those periods. The $N_{sub\text{-}2}$ were calculated from the difference in the particle number concentrations measured with PSM at two different DEG saturation ratios, 1.0 slpm (D_{50}: 1.3 nm) and 0.2 slpm (D_{50}: 2.0 nm). Assuming a nucleation mode with lognormal distribution of the 1.6 nm median diameter and 1.2 standard deviation, $N_{sub\text{-}2}$ represents 70% of the total concentration of this nucleation mode. $N_{sub\text{-}2}$ represents neutral particles, charged particles, and air ions between 1 and 2 nm. Because all of these particles can act as embryos for new particle formation in the atmosphere, we did not differentiate neutral particles, charged particles, and air ions in our study. We compared $N_{sub\text{-}2}$ and $N_{sub\text{-}3}$ during 12–14 August 2011 when both $N_{sub\text{-}3}$ and $N_{sub\text{-}2}$ data sets were available (Figure 2). The $N_{sub\text{-}2}$ closely followed a similar diurnal variation as the $N_{sub\text{-}3}$ (Figure 2a), but there was no clear linear correlation between $N_{sub\text{-}2}$ and $N_{sub\text{-}3}$. The $N_{sub\text{-}2}$ were also smaller than the $N_{sub\text{-}3}$ for 96% of all data points (Figure 2b), as one would expect. Because $N_{sub\text{-}2}$ and $N_{sub\text{-}3}$ closely followed the same diurnal variation, we used $N_{sub\text{-}2}$ to show diurnal patterns in Figure 3. In the present study, $N_{sub\text{-}2}$ were annotated where they were used (instead of $N_{sub\text{-}3}$). For the statistical analysis of $N_{sub\text{-}3}$, the 4 days with $N_{sub\text{-}2}$ were not included.

Gas phase H_2SO_4 concentrations [H_2SO_4] were measured with an atmospheric pressure chemical ionization mass spectrometer (CIMS) using nitrate ions as reagent [*Eisele and Tanner*, 1993; *Erupe et al.*, 2010; *Kanawade et al.*, 2011]. Our CIMS can measure [H_2SO_4] down to the 5×10^4 cm^{-3} with an integration time of 1 minute and an uncertainty of a factor of 2 (*Yu et al.*, 2012). A proton transfer time of flight mass spectrometer (PTR-TOF-MS, Ionicon) was deployed to measure concentrations of key biogenic VOCs including isoprene (ion mass to charge ratio m/z 69), methylvinylketone and methacrolein (isomers, m/z 71), acetaldehyde (m/z 45), formic acid (m/z 47), acetic acid (m/z 61), methanol (m/z 33), acetone (m/z 59), and monoterpenes (m/z 137), and anthropogenic VOCs such as benzene (m/z 79) and toluene (m/z 93), and xylenes (m/z 107). Sulfur dioxide (SO_2), ozone (O_3), nitrogen oxides (NO and NO_2), and total reactive nitrogen species (NO_y) concentrations were measured with Thermo Environmental Instruments (model 43i-TLE, 49i, and 42i, respectively). Carbon monoxide (CO) was measured with a CO-23r Analyzer (Los Gatos Research). In situ meteorological parameters including wind speed, wind direction, relative humidity (RH), and temperature were measured (at 1 Hz) during the

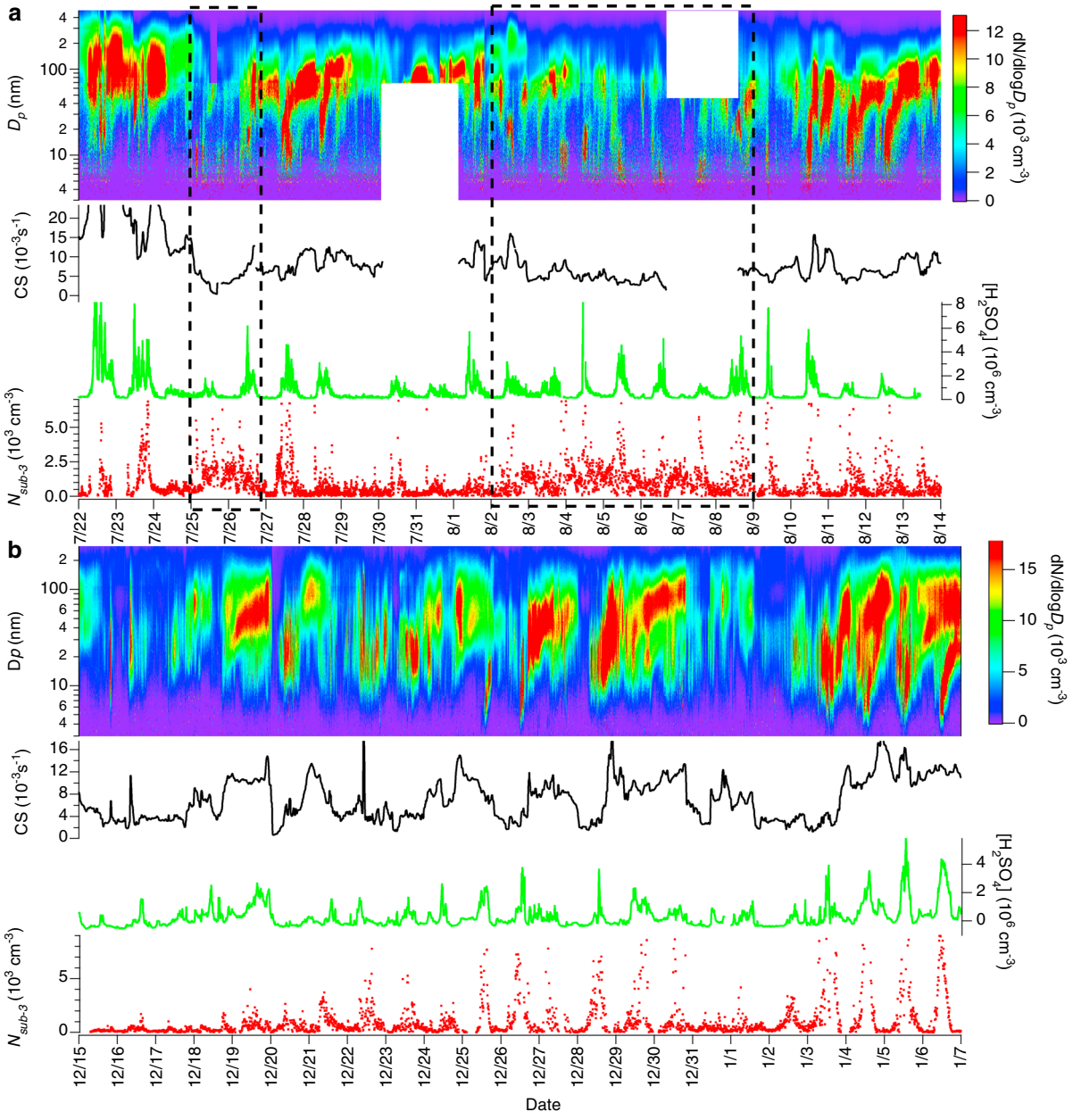

Figure 3. The measured particle size distributions from 3 to 478 nm (5 min median), condensation sink CS (5 min median, black), H_2SO_4 concentrations [H_2SO_4] (1 min median, green), and sub-3 nm particle number concentrations N_{sub-3} (5 min median, red dots) at (a) Brookhaven from 22 July to 13 August 2011 and (b) Kent from 15 December 2011 to 6 January 2012. There were no nano-SMPS measurements from 30 to 31 July 2011 and no SMPS measurements from 6 to 8 August 2011 at Brookhaven. Dashed boxes in Figure 3a highlight the periods of the nighttime events which occurred at Brookhaven when the site was influenced by the marine air masses.

IOP study period but not continuously. Thus, we also used hourly data of temperature, RH, mixing layer height, rain fall, solar flux, wind speed, and wind direction retrieved from the NOAA Hybrid Single-Particle Lagrangian Integrated Trajectory (HYSPLIT) model [*Draxler and Rolph*, 2003] to complement the in situ meteorological measurements. 72 h backward trajectories were calculated from the HYSPLIT model at a height of 500 m at the hourly base for the entire IOP period.

The second measurements were made in Kent, Ohio. The sampling was made from the top floor (15 m above the ground level) of Williams Hall at the Kent State University's Kent campus (41.158°N, 81.368°W, 320 m above sea level; indicated by green star in Figure 1b). Kent is a small college town surrounded by three urban cities in near distance: approximately 60 km southeast of Cleveland, 30 km east of Akron, 100 km west from Pittsburgh.

A large number of coal-burning power plants are located within 300 km (http://www.epa.gov/airdata/), so this site is affected by high-sulfur plumes year around. Kent is also a very treed town and has local biogenic VOC emissions from various Maple, Beech, and Birch trees. In the present study, we report $N_{sub\text{-}3}$, $[H_2SO_4]$, and particle size distribution from 3 to 478 nm ($N_{3–478}$) measured with PSM, CIMS, and two SMPSs (TSI DMA 3085 with CPC3776; TSI DMA 3081 with CPC 3772), respectively, over 23 days from 15 December 2011 to 6 January 2012. The $N_{3–478}$ and $N_{sub\text{-}3}$ calculations for the Kent data followed the same procedure as that used for the Brookhaven data. The correlation coefficient (R^2) was 0.97 with a slope of 1.06 for the total particle concentrations in the overlapped size range of 10–64 nm measured by the nano-SMPS and long-SMPS. During the measurement, the ambient air with a flow rate of ~3000 slpm was drawn into a 1.5 m long and 10.16 cm diameter air duct. The PSM was directly connected to the air duct via a 4 cm long and 0.64 cm diameter tube. The transport loss in front of the PSM was estimated to be 6% and 22% for 3 nm and 1 nm particles, respectively. An averaged transport loss of 14% was used in the $N_{sub\text{-}3}$ calculation. During the sampling period, HYSPLIT model calculations (at a height of 500 m) indicated that the prevailing wind direction was westerly and the site mostly had continental air masses that originated predominately from northwest or southwest. Long-term, semicontinuous measurements of aerosol size distributions (2006–2013 for over 8 years), H_2SO_4 and NH_3 (2009–2013), have been made at this site [*Benson et al.*, 2010; *Erupe et al.*, 2010; *Kanawade et al.*, 2012]. And, recent measurements of amines were also reported from this site [*Yu and Lee*, 2012]. Kent thus represents one of the very few sites in the Northern America, where the long-term semicontinuous observations of aerosol size distributions and nucleation precursors were conducted.

3. Results and Discussion

Figure 3 shows $N_{sub\text{-}3}$, $[H_2SO_4]$, condensation sink (CS) and particle size distribution at Brookhaven and Kent. CS is the sink rate at which H_2SO_4 molecules condense on preexisting aerosol particles [*Erupe et al.*, 2010]. The lowest $N_{sub\text{-}3}$ (which is the background $N_{sub\text{-}3}$, as defined in this study) usually occurred during the nighttime. The background $N_{sub\text{-}3}$ was $230 \pm 200\ cm^{-3}$ (median and 1 standard deviation) at Brookhaven and $180 \pm 130\ cm^{-3}$ in Kent; thereby, they were comparable at both sites.

We defined a sub-3 nm particle formation event when there was a burst of sub-3 nm particles, as indicated by a substantial $N_{sub\text{-}3}$ (higher than $1000\ cm^{-3}$) continuously for more than 4 h. On the other hand, a NPF event was defined when sub-3 nm particles underwent a continuous growth to large sizes for a few hours, as indicated by a distinctive "banana-shaped" contour plot of particle size distribution. Thus, a "NPF event" differs from a "sub-3 nm particle event". As will be discussed in detail below, not all of the sub-3 nm particle events led to NPF events at both sites, which is one of our main conclusions.

3.1. Sub-3 nm Particles in Brookhaven, New York: During the Day and Nighttime

3.1.1. Daytime Events

At Brookhaven, daytime sub-3 nm particle events were observed on 20 out of 23 days, and nighttime events during the 6 nights (Figure 3a). The $N_{sub\text{-}3}$ observed during the daytime events were $1800 \pm 630\ cm^{-3}$, substantially higher than those during the nonevent days ($450 \pm 220\ cm^{-3}$ during the daytime). The daytime sub-3 nm particle events were clearly absent on the days when $[H_2SO_4]$ were low ($< 1.0 \times 10^6\ cm^{-3}$; such as 24 July, 29 July, and 31 July). Diurnal variations of the median $N_{sub\text{-}3}$ with and without daytime events are shown in Figure 4a (red line and grey line, respectively). During the daytime events, the $N_{sub\text{-}3}$ exceeded $1000\ cm^{-3}$ starting from 8 A.M. local time, coincident with the H_2SO_4 formation. And, there was no time delay between the $N_{sub\text{-}3}$ and $[H_2SO_4]$ peaks, or the time delay was shorter than 10 min, which was the time resolution of synchronized SMPS measurements. On the other hand, there was a substantial time delay between $N_{3\text{-}10}$ and the $[H_2SO_4]$ peaks (typically 2 h). The $N_{sub\text{-}3}$ then decreased instantly with the decrease of $[H_2SO_4]$ and dropped to less than $500\ cm^{-3}$ around 6 P.M. Thus, the formation of sub-3 nm particles was directly related to the formation of H_2SO_4. These results indicate that the daytime sub-3 nm particles were present only at high $[H_2SO_4]$, and they were absent otherwise.

The production of sub-3 nm particles was not suppressed by large particles, and the measured CS were moderately high during the sub-3 nm particle events ($> 1.0 \times 10^{-2}\ s^{-1}$; Figure 3a). This result indicates that at high $[H_2SO_4]$ conditions, sub-3 nm particles were formed regardless of CS conditions. However, for most of the time, these sub-3 nm particles did not grow larger to lead to any significant NPF. Distinctive NPF events

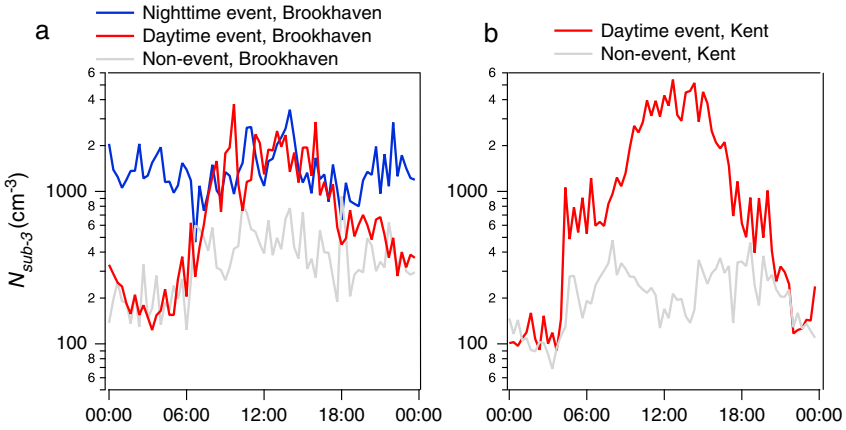

Figure 4. Diurnal variations of sub-3 nm particle concentration ($N_{sub\text{-}3}$) at (a) Brookhaven and (b) Kent. The red lines represent the median of 20 min concentrations for the days with daytime events, the blue line for the days with nighttime events, and the grey line for nonevent days.

were only observed for 4 days during the entire 23 days of the sampling period (Figure 3a), while there were 20 days of the sub-3 nm particle events.

The atmospheric conditions commonly found during the four NPF events at the Brookhaven site included (i) continental air masses originated from northwest across the United States and Canada (red trajectories in Figure 1a), (ii) [H_2SO_4] higher than 1.0×10^6 cm^{-3}, (iii) mixing layer heights higher than 1500 m, CS lower than 6×10^{-3} s^{-1}, relatively low RH (40–50%) at the noontime, and (iv) large temperature diurnal variations. Previously, *Nilsson et al*. [2001] suggested that strong solar radiation and boundary layer mixing/convection (and thus higher mixing height) may trigger a NPF event in the daytime. Therefore, our observation is consistent with *Nilsson et al*. [2001] that NPF events are often accompanied by higher mixing layer heights. Although the above five conditions were commonly observed during the four NPF events, these conditions alone still were not sufficient for NPF. For the growth of these sub-3 nm particles, other condensable organic compounds were also involved, because the growth rates (GR) derived from the condensation of H_2SO_4 [*Nieminen et al*., 2010] accounted for only 0.5–2.2% of the measured GR during these NPF events.

During the NPF events, it usually took 10–12 h for sub-3 nm particle to grow to ~ 70 nm. The measured GR in the particle size range between 3 and 10 nm were between 0.64 and 2.49 nm h^{-1}, in the continental air masses at Brookhaven. During 25–26 July and 2–8 August 2011 (indicated by dashed boxes in Figure 3a), this site was mainly influenced by marine air masses. In these marine air masses, the sub-3 nm particles grew only to ~ 10 nm and appeared continuously for 2–4 h around the noon, but they disappeared as soon as [H_2SO_4] began to drop afterward (Figure 3a). Synoptic situation analysis during NPF events in Finland [*Sogacheva et al*., 2008] previously suggested that cloudiness, often associated with frontal passages, decreased the amount of solar radiation and in turn reduced the growth of new particles. In the present study we did not have cloudiness data during our measurement periods. Instead, we checked hourly solar radiation in the marine air mass prevailing days, which is found to be as high as those in the continental air mass prevailing days. Furthermore, the noontime peak height and the duration of [H_2SO_4] in the marine air masses were comparable to those during the four NPF events found in the continental air masses. The CS in the marine air masses (~ 4.8×10^{-3} s^{-1}) were lower than those in the continental air masses (~ 9.7×10^{-3} s^{-1}). Hence, these factors (solar radiation, H_2SO_4, and CS) together actually should have provided a better condition for NPF in the marine air masses than in the continental air masses. This implies again that the growth of sub-3 nm particles needed some gas phase precursors other than H_2SO_4 (likely organics); while these precursors were present in the continental air masses, they were somehow missing in the marine air masses at the Brookhaven site.

During the daytime NPF events which had clear "banana-shaped" contour plots, we calculated nucleation rate (J) using the particle growth and nucleation (PARGAN) inversion model [*Erupe et al*., 2010; *Kanawade et al*., 2012; *Verheggen and Mozurkewich*, 2006]. The PARGAN-calculated J (J_{PARGAN}) ranged from 0.4 to 1.8 cm^{-3} s^{-1} (Table 1). The J_{PARGAN} values were based on the SMPS-measured aerosol size distributions, as the PARGAN uses a general dynamic equation to derive J; on the other hand, $N_{sub\text{-}3}$ were based on the differences in particle number

Table 1. The Median and 1 Standard Deviation Values of Condensation Sink (CS), H_2SO_4 Concentration [H_2SO_4], Sub-3 nm Particle Number Concentration ($N_{sub\text{-}3}$), and Nucleation Rates (J) During the Daytime and Nighttime Events and Non-Event Nights at Brookhaven, New York, and Kent, Ohio[a]

Site	Airmass Type	Date	CS (10^{-3} s^{-1})	[H_2SO_4] (10^6 cm^{-3})	$N_{sub\text{-}3}$(10^3 cm^{-3})	J (cm^{-3} s^{-1})
			Nighttime Events			
Brookhaven	Marine	25 Jul 2011	3.7 ± 0.6	0.19 ± 0.05	2.1 ± 0.8	1.3 ± 2.1
		2 Aug 2011	5.1 ± 1.9	0.36 ± 0.16	1.5 ± 0.3	1.1 ± 2.9
		3 Aug 2011	5.1 ± 0.7	0.17 ± 0.04	1.4 ± 0.6	1.0 ± 3.2
		4 Aug 2011	5.0 ± 0.8	0.32 ± 0.08	1.5 ± 0.5	1.2 ± 3.8
		5 Aug 2011	3.6 ± 0.9	0.19 ± 0.09	1.0 ± 0.5	0.51 ± 2.4
		6 Aug 2011		0.21 ± 0.08	1.3 ± 0.5	
		Median	4.5	0.24	1.5	1.0
			Nonevent Nights			
Brookhaven	Continental	27 Jul 2011	11.6 ± 0.6	0.15 ± 0.05	0.16 ± 0.14	0.26 ± 1.4
		28 Jul 2011	11.6 ± 0.5	0.16 ± 0.05	0.20 ± 0.17	0.34 ± 1.7
		29 Jul 2011	7.1 ± 1.0	0.20 ± 0.06	0.34 ± 0.30	0.32 ± 1.5
		1 Aug 2011	7.6 ± 1.3	0.20 ± 0.09	0.26 ± 0.19	0.24 ± 1.7
		9 Aug 2011	7.8 ± 0.9	0.16 ± 0.04	0.24 ± 0.14	0.18 ± 1.2
		10 Aug 2011	9.2 ± 2.3	0.26 ± 0.11	0.16 ± 0.11	0.17 ± 1.2
		12 Aug 2011	6.3 ± 0.1	0.14 ± 0.02	0.16 ± 0.12	0.13 ± 1.5
		13 Aug 2011	10.1 ± 0.5	0.15 ± 0.06	0.19 ± 0.14	0.21 ± 1.5
		Median	8.9	0.18	0.20	0.23
Kent	Continental	1 Jan 2012	3.3 ± 0.2	0.20 ± 0.03	0.19 ± 0.08	0.10 ± 0.11
		15 Dec 2011	3.2 ± 0.7	0.11 ± 0.07	0.09 ± 0.04	0.04 ± 0.06
		16 Dec 2011	3.6 ± 0.2	0.30 ± 0.14	0.09 ± 0.03	0.05 ± 0.06
		17 Dec 2011	6.3 ± 1.9	0.76 ± 0.28	0.17 ± 0.14	0.16 ± 0.19
		31 Dec 2011	7.1 ± 1.7	0.47 ± 0.23	0.19 ± 0.18	0.18 ± 0.28
		25 Dec 2011	4.1 ± 1.6	0.48 ± 0.14	0.18 ± 0.09	0.10 ± 0.14
		30 Dec 2011	5.2 ± 1.1	0.34 ± 0.09	0.24 ± 0.13	0.19 ± 0.20
		4 Jan 2012	14.8 ± 2.2	0.89 ± 0.37	0.15 ± 0.13	0.19 ± 0.17
		Median	6.1	0.47	0.17	0.13
			Daytime Events With NPF			
Brookhaven	Continental	27 Jul 2011	5.6 ± 1.3	1.21 ± 0.43	3.6 ± 2.9	1.5 ± 1.8
		10 Aug 2011	4.7 ± 0.9	2.49 ± 1.54	4.0 ± 3.8	1.8 ± 2.4
		11 Aug 2011	4.3 ± 0.5	0.56 ± 0.23	2.1 ± 1.6	0.8 ± 0.9
		12 Aug 2011	5.4 ± 0.5	0.64 ± 0.33	1.0 ± 0.9	0.4 ± 0.3
		Median	5.0	1.23	2.7	1.1
Kent	Continental	3 Jan 2012	2.8 ± 1.2	1.32 ± 0.88	7.7 ± 5.3	1.1 ± 1.3
		4 Jan 2012	10.1 ± 0.8	1.77 ± 0.75	12.8 ± 5.2	1.3 ± 1.5
		5 Jan 2012	9.8 ± 1.0	3.25 ± 1.10	9.1 ± 4.3	1.4 ± 0.6
		6 Jan 2012	11.0 ± 0.9	3.33 ± 1.07	19.3 ± 7.0	1.6 ± 3.7
		25 Dec 2011	7.9 ± 1.0	1.99 ± 0.66	7.4 ± 5.4	0.9 ± 2.9
		Median	8.0	2.10	9.0	1.3

[a]The J values shown here are formation rates of sub-3 nm particles (J') derived from equation (1) for the nighttime and the J_{PARGAN} during the distinctive NPF events. For the 6 August 2011's nighttime event, CS and J are not provided here, due to incomplete SMPS size distribution data, and the $N_{sub\text{-}2}$ is provided (instead of $N_{sub\text{-}3}$) from the PSM measurements using different DEG saturator flows.

concentrations measured with PSM and SMPS. A correlation analysis between J_{PARGAN} and $N_{sub\text{-}3}$ during the four NPF events is shown in Figure 5. These comparisons indicate that during NPF events, higher J_{PARGAN} were usually associated with higher $N_{sub\text{-}3}$. But within a single NPF event, there was no clear correlation between J_{PARGAN} and $N_{sub\text{-}3}$.

3.1.2. Nighttime Events

Nighttime events were observed at Brookhaven, only when prevailing winds were from the ocean (25 July and from 2–6 August). The occurrence of such nighttime sub-3 nm particles in specific air masses again demonstrates that sub-3 nm particles were not always present, consistent with the daytime results discussed in the above section.

A typical example of the air mass movements during these nighttime events is shown as blue trajectories in Figure 1a. The measured $N_{sub\text{-}3}$ were 1500 ± 400 cm^{-3} during the nighttime sub-3 nm particle events, but these nocturnal sub-3 nm particles usually did not grow larger (Figure 3a). Because of these nighttime events, the diurnal variation of $N_{sub\text{-}3}$ on these days was not as clear as other days, which did not have the nighttime events (blue line, Figure 4a). At the Brookhaven site when it was influenced by the continental air masses, the nighttime $N_{sub\text{-}3}$ were also very low (200 ± 160 cm^{-3} s near the background level). These low concentrations were also comparable to the cases seen at the winter continental Kent site (as will be discussed in the

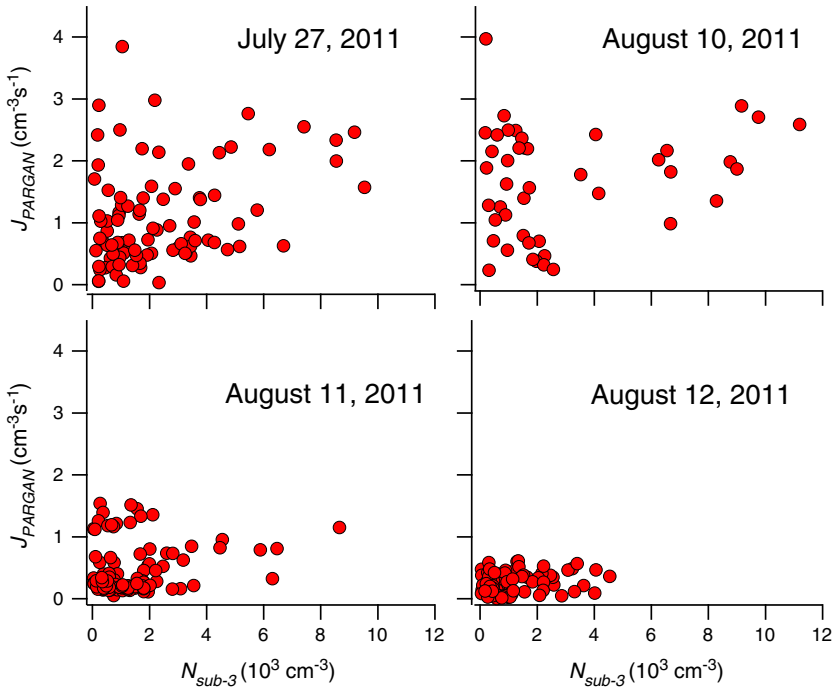

Figure 5. Correlations between J_{PARGAN} and N_{sub-3} during the four NPF events observed at the Brookhaven site.

following section). Therefore, these nighttime sub-3 nm particle events were likely associated with the marine air masses (as opposed to the continental air masses), and they were not due to summer-winter variations.

Figure 6 shows the time series of the N_{sub-3}, H_2SO_4, VOCs, other key trace gas concentrations, and particle size distributions measured in the marine air masses (25 July and 2–6 August). These nighttime sub-3 nm particle events occurred under the conditions with relatively low CS (~ 4.5×10^{-3} s^{-1}; N_{sub-3} accounted for 30–50% of N_{tot}), high RH (~ 80%), and moderate hourly fluctuations of RH, temperature, and mixing layer height. The measured [H_2SO_4] (~ 2.4×10^5 cm^{-3}) during the nighttime events were not statistically higher than during the nonevent nights (~ 1.8×10^5 cm^{-3}), but they were 1 order of magnitude lower than those during the daytime sub-3 nm particle events (~ 1.5×10^6 cm^{-3}). From our limited data set, the nighttime N_{sub-3} found in the marine air masses did not seem to have a clear correlation with low tides (Figure 6a), unlike the results reported from Mace Head in the western Ireland where strong particle formation events were frequently observed during the low tides [*Lehtipalo et al.*, 2010; *Vana et al.*, 2008].

To verify if the measured nighttime N_{sub-3} particles were "transported over" from the residual sub-3 nmparticles formed during the previous daytime or not, we have performed simple coagulation calculations. In these calculations, the initial N_{sub-3} was set as 1500 cm^{-3} and a median size as 2 nm, to represent the typical nighttime event condition. The SMPS-measured total number particle concentrations were between 3000 and 6000 cm^{-3} during the nighttime events (e.g., 9:00 P.M. to 6:00 A.M., 3–6 August). Our calculation results indicate that the N_{sub-3} would have decreased to less than 10% of the originally prescribed level within 20 min if there was not a continuous supply of nucleation precursors. Therefore, these observed nighttime sub-3 nm particles were not transported over from the prior daytime sub-3 nm particles; instead, they were formed at in situ at night from some unidentified nucleation precursors that were present in the marine air masses.

We further calculated formation rate J' (or evaporation rate, in the case of a negative value of J') of the nighttime sub-3 nm particles, by assuming that there was no significant nanoparticle growth across 3 nm (as seen from Figures 3a and 6a) and based on the following relationship adopted from *Dal Maso et al.* [2005] and *Kulmala et al.* [2001]:

$$J' = \frac{dN_{sub-3}}{dt} + CoagS_{2nm} \times N_{sub-3} \quad (1)$$

where $CoagS_{2nm}$ is the coagulation sink of sub-3 nm particles (again, a 2 nm median size was assumed here), due to coagulation with larger particles (that is, those in the size range from 3 to 478 nm measured by SMPS).

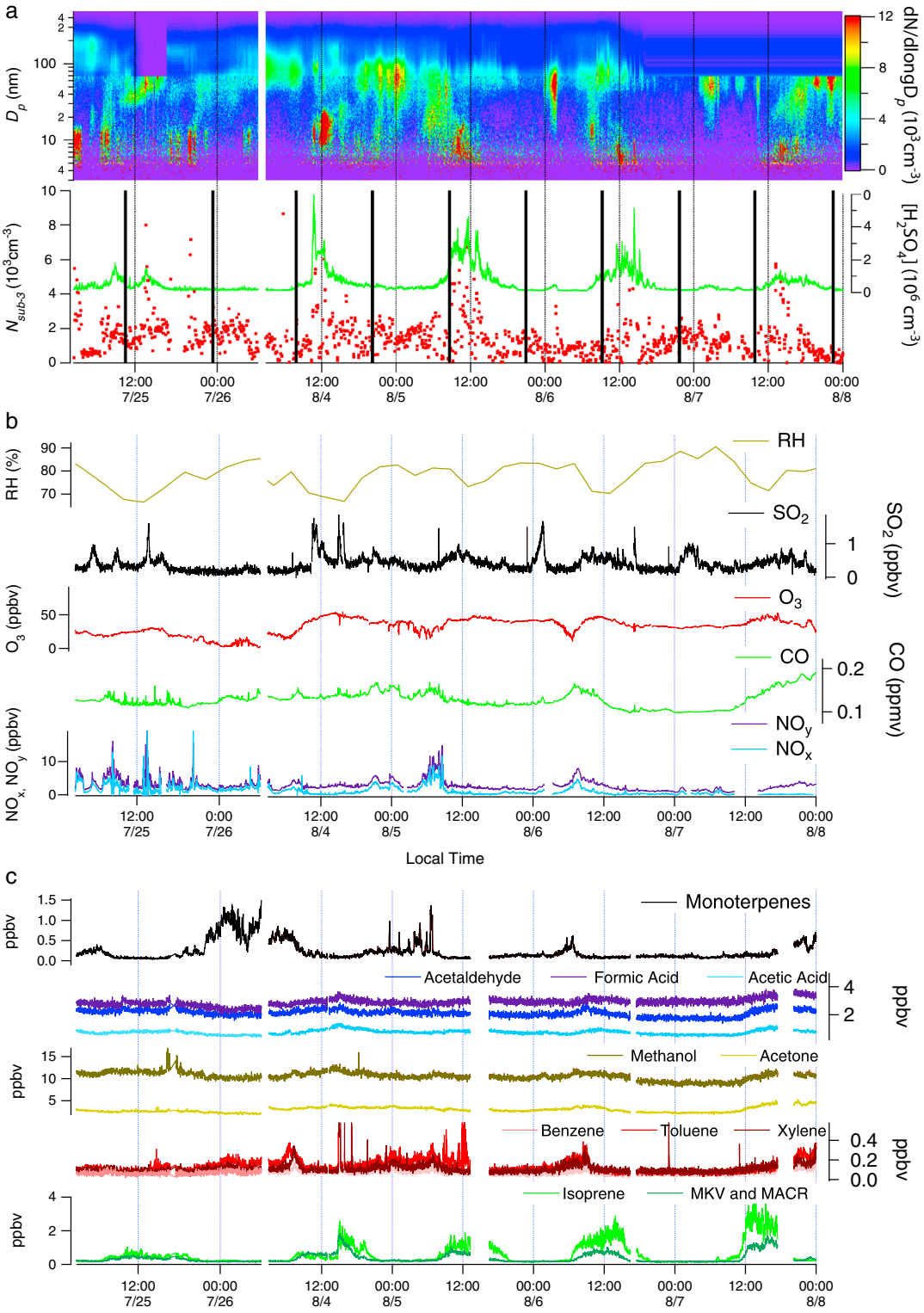

Figure 6. The measured particle sizes and concentrations of sub-3 nm particles and key gas phase species at Long Island site from 25 to 27 July and from 4 to 7 August 2011 when clear nighttime events were observed. (a) Particle size distributions from 3 to 478 nm, [H_2SO_4] (green line) and N_{sub-3} (red dots). Low tide times are shown as vertical black lines. (b) RH (grey), SO_2 (black), O_3 (red), CO (green), NO_x (light blue), and NO_y (dark violet). (c) VOCs measured by PTR-TOF-MS including monoterpenes (m/z 137; black), acetaldehyde (m/z 45; blue), formic acid (m/z 47; dark violet), acetic acid (m/z 61; light blue), methanol (m/z 33; olive), acetone (m/z 59; gold), benzene (m/z 79; pink), toluene (m/z 93; red), xylenes (m/z 107; brown), isoprene (m/z 69; green), and MVK + MACR (m/z 71; dark green).

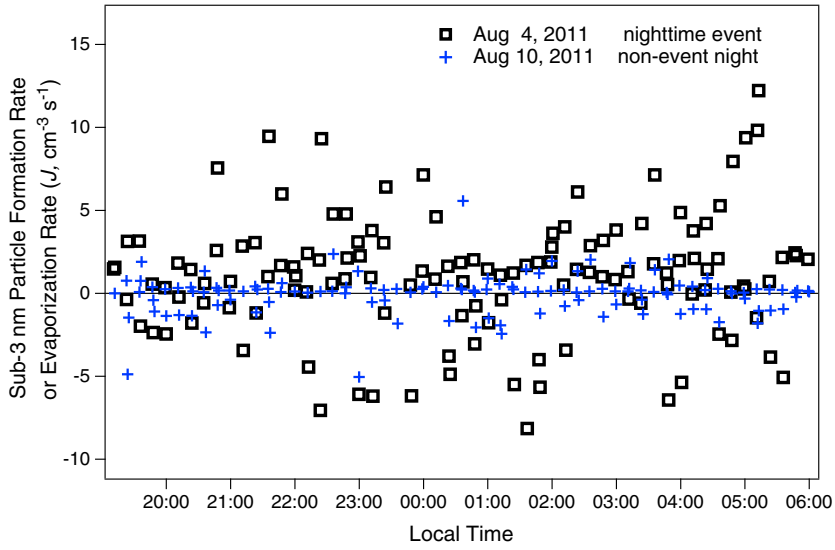

Figure 7. The calculated formation rate (or vaporization rate, in the case of the negative value) of sub-3 nm particles (J') during a nighttime event on 4 August 2011 (black squares) and during a nonevent night on 10 August 2011 (blue crosses).

Figure 7 shows an example of J' derived for an event (4 August) versus a nonevent night (10 August). The J' during the eventnight ranged from -7 to 10 $cm^{-3}\,s^{-1}$ with a median value of $1.2 \pm 3.8\,cm^{-3}\,s^{-1}$. The net formation or evaporation of sub-3 nm particles never lasted longer than 1 h. So the overall effect is that $N_{sub\text{-}3}$ remained relatively constant in the nighttime atmosphere. Because there was a net particle loss due to coagulation in the night, the overall J' throughout the whole night was positive. In other words, to maintain a nearly constant presence of sub-3 nm particles in the nocturnal atmosphere, there must have been a constant source of nucleation precursors to offset particle loss due to coagulation and evaporation. During the nonevent night, the J' were 1 order of magnitude lower ($0.17 \pm 1.2\,cm^{-3}\,s^{-1}$) than during the event night, and they were randomly scattered within the $\pm 2\,cm^{-3}\,s^{-1}$ range.

The median and standard deviation values of J' during each nighttime event and some nonevent nights are shown in Table 1. At the Brookhaven site, the derived J' during the nighttime sub-3 nm particle events found in the marine air masses ($1.0 \pm 2.9\,cm^{-3}\,s^{-1}$) were consistently higher than those during the nonevent nights in the continental air masses ($0.23 \pm 1.5\,cm^{-3}\,s^{-1}$). The J' during the nighttime events were even comparable to the J_{PARGAN} derived from the daytime NPF events ($1.1 \pm 1.4\,cm^{-3}\,s^{-1}$) at the same site, indicating that the formation of nighttime sub-3 nm particles were indeed substantial.

3.2. Sub-3 nm Particles in Kent, Ohio: Only During the Daytime

There were daytime sub-3 nm particles on 17 days out of 23 days of the observation period at the Kent site. Despite the different sampling seasons (summer in Brookhaven versus winter in Kent), the characteristic features of the daytime $N_{sub\text{-}3}$ were in fact strikingly similar, as discussed in this section. However, there was not a single nighttime event during this observation period in Kent (Figure 3b), unlike at the Brookhaven site.

The median $N_{sub\text{-}3}$ during daytime sub-3 nm particle events was $3700 \pm 1300\,cm^{-3}$ 1 order of magnitude higher than those during the nonevent days ($200 \pm 110\,cm^{-3}$). Daytime sub-3 nm particle events were absent on clean days when $[H_2SO_4]$ were low ($< 1.0 \times 10^6\,cm^{-3}$; 15–18 December 2011 and 31 December 31 to 1 January 2012). Diurnal variations of $N_{sub\text{-}3}$ with and without daytime events are shown in Figure 4b (red line and grey line, respectively). Distinctive banana-shaped NPF events were observed only for 5 days in Kent (Figure 3b), although there were 17 days of sub-3 nm particle events.

The measured $N_{sub\text{-}3}$, $N_{3\text{-}10}$, CS, $[H_2SO_4]$, and particle size distributions on a typical NPF event day (17 January 2012) at the Kent site are shown in Figure 8. The $N_{sub\text{-}3}$ started to increase from the background level ($\sim 200\,cm^{-3}$) at ~7 A.M., when $[H_2SO_4]$ started to increase from $4 \times 10^5\,cm^{-3}$. After that, both $N_{sub\text{-}3}$ and $[H_2SO_4]$ increased and exceeded $2000\,cm^{-3}$ and $1 \times 10^6\,cm^{-3}$, respectively, around 9 A.M. The presence of

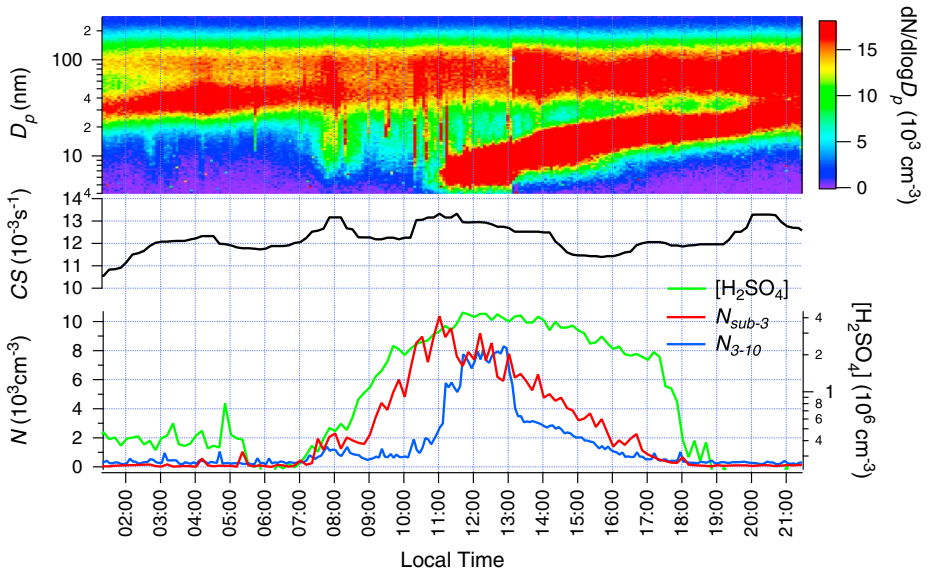

Figure 8. The measured particle size distribution, [H_2SO_4], *CS*, $N_{sub\text{-}3}$, and $N_{3\text{-}10}$ on a typical NPF event day (17 January 2012) in Kent.

particles in the size range from 3 to 200 nm (corresponding CS 1.2–1.3 × 10^{-2} s^{-1}) did not suppress the formation of sub-3 nm particles. The $N_{sub\text{-}3}$ reached its maximum of 9000 cm^{-3} at ~ 11 A.M. (followed by a typical banana plot), after which $N_{sub\text{-}3}$ began to decrease slowly and $N_{3–10}$ increased rapidly. There was a time lag of ~ 2 h between the $N_{sub\text{-}3}$ and $N_{3–10}$ peaks. The [H_2SO_4] maximum appeared around 12 P.M., while the [H_2SO_4] dropped to below 1 × 10^6 cm^{-3} around 6 P.M., $N_{sub\text{-}3}$ also decreased to less than 1000 cm^{-3} at nearly the same time.

GR derived for particles in the particles size range from 3 to 10 nm were 2.6–4.7 nm h^{-1}, during the five NPF events in Kent. These GR values were quite similar to those reported for winter seasons from earlier long-term observations (2006–2010) at the same site: 4.2 ± 0.3 nm h^{-1} [*Erupe et al.*, 2010; *Kanawade et al.*, 2012]. The calculated GR from the condensation of H_2SO_4 (1.3–3.3 × 10^6 cm^{-3}) alone accounted only for 2.5–3.5% of the observed GR, also similar to the previous report [*Erupe et al.*, 2010]. The J_{PARGAN} were 0.9–1.6 cm^{-3} s^{-1}, consistent with the average J_{PARGAN} of 1.0 ± 0.9 cm^{-3} s^{-1} in winter reported earlier from the same site [*Kanawade et al.*, 2012].

The NPF events took place in Kent, when there was a mixing layer height lower than 600 m, and the solar flux was higher than 300 W m^{-1} in air masses traveling from far north with a moderate [H_2SO_4] between 1.0 × 10^6 and 4.0 × 10^6 cm^{-3} or in stagnant air masses with [H_2SO_4] higher than 4.0 × 10^6 cm^{-3} (red trajectories in Figure 1b). These conditions favorable for NPF were derived from back trajectory calculations during 23 days in winter, and during that period air masses traveled predominately from northwest or southwest. These conditions were thus different from the previous long-term observations over a 4 year period (2006–2010) at the same site, which showed that NPF events were often associated with air masses from east and southeast where numerous large size power plants are located [*Kanawade et al.*, 2012].

For the cases in which daytime sub-3 nm particle events were not followed by the signature banana shape, the growth was affected by abrupt changes in wind direction, or the particle growth was suppressed by preexisting large particles (e.g., CS was around 10^{-2} s^{-1} on 29 and 30 December). It seemed that the presence of large particles (i.e., high CS condition) did not inhibit the sub-3 nm particle burst, but CS might have suppressed their subsequent growth to larger than 3 nm, due to the competition between the uptake of condensable vapors and the scavenging of sub-3 nm particles by large particles. Another possibility is that condensable vapors may have not been enough for the growth of sub-3 nm particles on some days. However, we did not measure VOCs in Kent, so we do not have evidence to support this hypothesis.

There was no nighttime sub-3 nm particle event in Kent during the 23 days of the observation period. The nighttime $N_{sub\text{-}3}$ were nearly negligible, 170 ± 160 cm^{-3}. The calculated *J'* (from equation (1)) were only

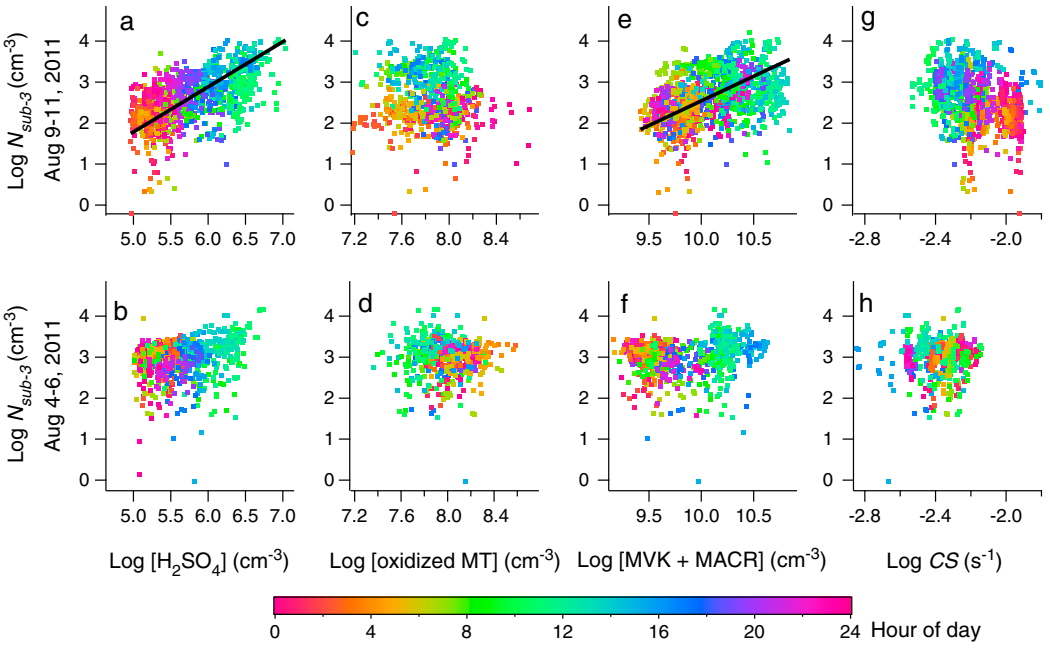

Figure 9. The correlations of Log N_{sub-3} versus Log [H_2SO_4], Log N_{sub-3} versus Log [oxidized MT], Log N_{sub-3} versus Log [MVK + MACR], and Log N_{sub-3} versus Log CS at Brookhaven in the marine air masses (4–6 August 2011) and the continental air masses (9–11 August 2011). Both daytime and nighttime data are included here; the colors indicate different hours of the day. Black solid lines indicate the linear fitting of the observation data. $N_{sub-3} = 2 \times 10^{-4} \times [H_2SO_4]^{1.1}$ ($R^2 = 0.34$, Figure 3a). $N_{sub-3} = 4 \times 10^{-10} \times [MVK + MACR]^{1.2}$ ($R^2 = 0.18$, Figure 3e).

0.13 ± 0.15 cm^{-3} s^{-1} at night, 1 order of magnitude lower than J_{PARGAN} (1.3 ± 2.0 cm^{-3} s^{-1}) that were derived during daytime NPF events. These results are different from the Brookhaven site where some nighttime sub-3 nm particle events were observed under the influences of marine air masses.

3.3. Possible Origin of Sub-3 nm Particles

We performed correlation analysis to see which aerosol precursors were correlated to the measured sub-3 nm particles. A linear regression between Log [H_2SO_4] and Log N_{sub-3} during 3 consecutive days in continental air masses at Brookhaven (9–11 August 2011 where only daytime events observed) had a slope of 1.1 and R^2 of 0.34 (Figure 9a). This R^2 was the highest, amongst all correlations between N_{sub-3} and gas phase species chosen in our analysis. If looking at only daytime data points during this period, R^2 ranged from 0.16 to 0.23 for the three daytime events (Figure 9a).

During another 3 consecutive days when the Brookhaven site was dominated by the marine air masses (4–6 August 2011 where both nighttime events and daytime events were observed), the linear correlation between Log [H_2SO_4] and Log N_{sub-3} was even weaker, and there was a group of nighttime data points located on the top-left corner (Figure 9b). This result reflects the fact that high concentrations of nighttime sub-3 nm particles in the coastal air masses were still maintained (~ 1000–3000 cm^{-3}) even with very low [H_2SO_4] of ~ 2×10^5 cm^{-3} during the nighttime. For the daytime and nighttime events only, R^2 were 0.32 and 0.09, respectively. The low correlations between Log [H_2SO_4] and log N_{sub-3} observed in our measurement are, in general, consistent with the low to moderate correlations reported in the Finland boreal forest, where the correlation coefficient R^2 between 1.5–2.0 nm nanoparticles and [H_2SO_4] was 0.35 and the R^2 between 0.9–1.5 nm particles and [H_2SO_4] was 0.58 [*Kulmala et al.*, 2013]. As suggested by *Kulmala et al.* [2013], the particle size range from 1 to 3 nm may include several subregimes of different nucleation mechanisms, not limited to the H_2SO_4–H_2O binary homogeneous nucleation. Therefore, the low correlations observed in our measurement imply that other gas precursors than H_2SO_4 also contributed to the formation of 1–3 nm particles.

There were some nighttime H_2SO_4 formation under high SO_2 conditions at Brookhaven, but these nighttime H_2SO_4 were not associated with sub-3 nm particle events. When there were SO_2 spikes (1–2 ppbv), the CIMS showed some elevated [H_2SO_4] up to 4×10^5 cm^{-3} (still 1 order of magnitude higher than the CIMS detection

limit), which occurred for a few minutes to half an hour around 1–3 A.M. and 7–9 P.M., accompanied with larger size particles (~ 50 nm). At this moment, we cannot explain these elevated nighttime H_2SO_4 observed during the night. We speculate that the nighttime H_2SO_4 were possibly formed from some aqueous or heterogeneous oxidation reactions with SO_2 on wet aerosols or cloud/fog droplets [*Harris et al*., 2013; *Lee et al*., 2008] or formed via *Criegee* intermediate reactions with SO_2 [*Mauldin et al*., 2012; *Paulson et al*., 1997]. In either cases, it was clear that the H_2SO_4 production in the atmosphere was not limited solely by OH radicals formed from photochemical reactions of ozone during the daytime. However, the H_2SO_4 production was also closely associated with SO_2 in high-sulfur plumes that were long range transported (evident by ~50 nm size particles). The same feature of the evening H_2SO_4 was also found during the long-range transported sulfur plumes in a mixed deciduous forest in the upper Michigan [*Kanawade et al*., 2011].

The total mixing ratios of monoterpenes (MT) measured with PTR-TOF-MS (including all isomers with m/z 137) were ~ 0.1 ppbv at noon and ~ 1 ppbv at night, and so they exhibited a diurnal variation opposite to the $N_{sub\text{-}3}$ in continental air masses at Brookhaven. Accordingly, the data points of $N_{sub\text{-}3}$ versus [oxidized MT] plots for the continental air masses randomly scattered (Figure 9c). The [oxidized MT] is the "apparent concentration" of monoterpene ozonolysis products calculated from k[MT][O_3]/CS, where k is reaction rate coefficient between α-pinene (the most abundant MT in the atmosphere [*Guenther et al*., 1995]) and O_3, and [MT] is the total monoterpene concentration. In the marine air masses at Brookhaven, [oxidized MT] were high at night and low during daytime, but the $N_{sub\text{-}3}$ were not correlated with [oxidized MT] (Figure 9d). In addition, [MT] were lower in coastal air masses than in continental air masses (a factor of 1.5–5). If monoterpenes were responsible for nighttime sub-3 nm particle formation, nighttime events should have occurred also in continental air masses at Brookhaven (and in Kent), but that was not the case. Therefore, we believe that monoterpene ozonolysis was an unlikely source of the nocturnal sub-3 nm particles observed at Brookhaven. This conclusion is different from the findings in the Hyytiälä boreal forests where there were abundant monoterpenes, and the measured sub-3 nm particles were closely correlated to oxygenated monoterpene compounds even during the nighttime [*Lehtipalo et al*., 2011; *Ortega et al*., 2012].

At Brookhaven, isoprene mixing ratios were between 2 and 5 ppbv around the noontime and decreased to ~ 0.1 ppbv at night. The peaks of the first generation oxidation products of isoprene, methylvinylketone, and methacrolein (MVK + MACR), usually appeared 1–3 h after the isoprene daytime peak. Correlation between (MVK + MACR) concentrations and $N_{sub\text{-}3}$ in the continental air masses was weak ($R^2 = 0.18$, Figure 9e). In the coastal air masses, the correlation was even weaker (Figure 9f), implying that isoprene and the first generation of isoprene oxidation products were also not responsible for the occurrence of the sub-3 nm particles.

There was also no link between nighttime events and anthropogenic pollutant tracers. NO_x ($NO + NO_2$) and NO_y are regarded as vehicle emission tracers. Their peaks were often, but not always, associated with 10–60 nm particles in the morning rush hours or around the midnight. Occasionally, nocturnal $N_{sub\text{-}3}$ spikes appeared in the air masses containing abundant NO_x and NO_y (e.g., from 9 P.M., 3 August to 1 A.M., 4 August). Such sub-3 nm particle spikes exhibited a distinctively different pattern from the usual nocturnal sub-3 nm particles that rather lasted all night long (Figure 6b). These sub-3 nm particle spikes were therefore formed from engine emissions of vehicles from the traffic. Benzene, toluene and xylenes (BTX), and CO are tracers of anthropogenic plumes. Particles from 40 to 100 nm were usually present in the plumes that contained high concentrations of BTX and CO. However, sub-3 nm particles were not observed in such plumes.

In the continental air masses, there was a trend of lower $N_{sub\text{-}3}$ that appeared at higher CS in the nighttime (Figure 9g). The high CS in the nighttime continental boundary layer reflects the presence of 60–100 nm large particles grown from the preceding daytime particle formation or transported from elsewhere. In the marine air masses, such a trend was not seen, and there was no anticorrelation between $N_{sub\text{-}3}$ versus CS for the CS range from 1×10^{-3} to 7×10^{-3} s^{-1} (Figure 9h). This led us to believe that the nighttime sub-3 nm particles were not a consequence of low CS.

3.4. Comparison With Previous Measurements of Sub-3 nm Particles at Other Sites

In this section, we compare our sub-3 nm particle measurements made at the coastal Brookhaven and the continental Kent sites with previous measurements of nano-CN at different sites from other groups. At Brookhaven and Kent, we did not observe the constant presence of sub-3 nm particles during the day and

Table 2. A Comparison of $N_{sub\text{-}3}$ (Mean Concentrations During the Entire Sampling Periods) Observed in This Study and at Other Locations in Recent Years[a]

			Mean Sub-3 nm Particle Concentration		
	Instruments	Sampling Period	All	Daytime (8 A.M. to 6 P.M.)	Nighttime (6 P.M. to 8 A.M.)
Kent, OH[b]	PSM/SMPS (1–3 nm)	15 December 2011to 6 January 2012	1,382 (50–2,700)	2,048	150
Brookhaven, NY[b]	PSM, SMPS (1–3 nm)	22 July to 13 August 2011	1,040 (40–3,800)	1,356	613
Mace Head, Ireland[c]	PH-CPC (1.3–3 nm)	13 June to 25 August 2008	3,490 (30–12,000)		
Hyytiälä, Finland[c]	PH-CPC (1.3–3 nm)	1–31 May 2008	8,950 (150–46,000)		
Hyytiälä, Finland[d]	PSM (0.9–2.1 nm)	14 March to 16 May 2011	10,684 (500–20,000)		

[a]The 5 and 95% interval values are shown in brackets.
[b]This study.
[c]*Lehtipalo et al.* [2010].
[d]*Kulmala et al.* [2013].

night, while other studies in the Hyytiälä boreal forest showed a more persistent presence of neutral clusters smaller than 2 nm [*Kulmala et al.*, 2007, 2013; *Lehtipalo et al.*, 2010, 2011]. Our PSM results showed that the daytime sub-3 nm particles were present with the elevated noontime peak of H_2SO_4, but there were some days in which $N_{sub\text{-}3}$ were significantly low (almost negligible) with low H_2SO_4 conditions during the day. The nighttime sub-3 nm particle events were seen only at the Brookhaven site, and they were clearly associated with the marine air masses and were not correlated to H_2SO_4 or biogenic VOCs. In the present study we cannot identify the nucleation precursors responsible for the nighttime sub-3 nm particles. On the other hand, nano-CN measured with DEG-SMPS at an urban site of Atlanta, Georgia, in summer 2009 showed some other characteristics [*Jiang et al.*, 2011a], which are also different from both the present study and the Hyytiälä boreal forest studies. They found that particles as small as 1 nm were only detected during daytime NPF events but not at other times.

Despite these differences in frequencies of sub-3 nm particle events that occurred at these different sites, the measured sub-3 nm particles overall were quite comparable. Table 2 shows a quantitative comparison of particle (or cluster) number concentrations in the sub-3 nm size range observed in the present study and those in different locations by other groups. $N_{sub\text{-}3}$ in Table 2 are mean sub-3 nm particle concentrations observed during the entire sampling periods in our study, as well as in other studies. In general, the $N_{sub\text{-}3}$ observed at our two sites were lower than recent measurements in other European sites, but they were all within the same order of magnitude. At the coastal Brookhaven site, the mean $N_{sub\text{-}3}$ was 1380 cm^{-3} (ranging from 50 to 2700 cm^{-3} for the 5–95% interval) for all 23 sampling days including both daytime and nighttime. At the continental Kent site the mean $N_{sub\text{-}3}$ was 1040 cm^{-3} (40–3800 cm^{-3}). At Mace Head, a coastal site of Ireland, the mean sub-3 nm nano-CN concentration (1.3–3 nm measured by PH-CPC) was reported to be 3490 cm^{-3} (30–12,000 cm^{-3}) [*Lehtipalo et al.*, 2010]. At the Hyytiälä boreal forest site, the mean nano-CN was reported to be 8950 cm^{-3} (150–46,000 cm^{-3}) [*Lehtipalo et al.*, 2010], and a more recent study with a PSM showed a mean sub-2 nm particle concentration (0.9–2.1 nm) of 10,680 cm^{-3} [*Kulmala et al.*, 2013]. These differences in particle number concentrations are probably due to different sampling locations and seasons, different instruments and methods used to derive nanometer size range particles (such as PH-CPC, PSM, and PSM/SMPS), and different particle size ranges of nano-CN reported in the cited studies. As discussed in the section 2, our method may have underestimated up to 60% of total particle number when the nucleation mode shifted from 3 nm to 1 nm. But this would not change the magnitude and the diurnal variations of sub-3 nm particles observed at our two sites.

A diurnal variation of $N_{sub\text{-}3}$ is an important characteristic that reflects nucleation mechanisms. At both sites of our study, $N_{sub\text{-}3}$ showed a maximum during the daytime and a minimum during the nighttime for most of the sub-3 nm particle event days (red lines, Figures 2a and 2b), except that sometimes the elevated nighttime sub-3 nm particles made a diurnal cycle appear less distinguishable in the marine air masses (blue line, Figure 2b). A recent study in the Hyytiälä boreal forest also showed a daytime maximum of sub-2 nm particles in March and May [*Kulmala et al.*, 2013]. But earlier observations at the same site found that nighttime concentration peaks occurred frequently in spring [*Lehtipalo et al.*, 2009, 2010, 2011; *Vanhanen et al.*, 2011], suggesting a possible link between the nanoparticle formation and the nighttime ozonolysis of monoterpenes and other biogenic VOCs. At the coastal site Mace Head, however, an opposite diurnal trend to our coastal site

was observed: Diurnal cycle was clear in marine air masses with a noontime or afternoon maximum, but there was no diurnal cycle when air masses passed over from the land areas [*Lehtipalo et al.*, 2010]. The reasons behind this difference are unknown at present and need further investigations.

Our calculated nucleation rates (J' derived from equation (1) and J_{PARGAN}) were compared with nucleation rates of 1.5 nm particles ($J_{1.5nm}$) retrieved from PSM measurements by scanning the DEG fluid flow rates at the Hyytiälä boreal forest site [*Kulmala et al.*, 2013]. The J_{PARGAN} (which represents the flux of nucleation critical clusters) during the daytime NPF events at our both sites were lower than the $J_{1.5nm}$ (1.5 nm was assumed as the critical cluster size based on *Kulmala et al.* [2013]) during the active aerosol formation periods reported from Hyytiälä. During the daytime NPF events, J_{PARGAN} ranged from 0.01 to 12 $cm^{-3}\,s^{-1}$, with median values of 1.1 and 1.3 $cm^{-3}\,s^{-1}$ at Brookhaven and Kent, respectively. During the periods of active aerosol formation at the boreal forest site, $J_{1.5nm}$ ranged from 0.1 to 40 $cm^{-3}\,s^{-1}$, with a median of 5.9 $cm^{-3}\,s^{-1}$. The J' calculated from equation (1) in the present study for the nighttime behaved quite differently and fluctuated between positive and negative values. During the nights without the presence of substantial sub-3 nm particles (and hence nonevents), the median J' were calculated to be 0.04–0.34 $cm^{-3}\,s^{-1}$, which are very close to $J_{1.5nm}$ of 0.2–0.4 $cm^{-3}\,s^{-1}$ during nonevent nights at Hyytiälä. However, in the marine air masses at Brookhaven, we observed a higher median J' of 0.5–1.3 $cm^{-3}\,s^{-1}$ during the nighttime sub-3 nm particles events.

$[H_2SO_4]$ were lower at our coastal Brookhaven site (ranging from 2×10^5 cm^{-3} during the nighttime at the background level to 1.6×10^6 cm^{-3} during an active NPF event) than at our Kent continental site (4.7×10^5 to 2.2×10^6 cm^{-3}). The background $[H_2SO_4]$ in nonevent days measured by CI-APi-TOF at Hyytiälä were around 2×10^5 to 7×10^5 cm^{-3}, in the same range as our background levels. The $[H_2SO_4]$ during active daytime events at Hyytiälä had a median value up to 8×10^6 cm^{-3} and were generally higher than our $[H_2SO_4]$ at both Kent and Brookhaven. When excluding the observed nighttime events which were associated with some unknown nucleation precursors in the marine air masses, we found that the correlation between J and $[H_2SO_4]$ was $J = 6.8 \times 10^{-6} \times [H_2SO_4]^{1.2}$ for our data shown in Table 1. This relationship is close to $J_{1.5nm} = 1.06 \times 10^{-7} \times [H_2SO_4]^{1.1}$ during the periods of the active NPF event period at Hyytiälä [*Kulmala et al.*, 2013]. These results are consistent with other studies which showed that the atmospherically observed J are in general proportional to $[H_2SO_4]$ with a first or second power [*Kulmala et al.*, 2004b].

4. Conclusions

We measured sub-3 nm particle concentrations in two distinct environments: a coastal site at Brookhaven in summer and an inland continental location in Kent in winter, for 23 days at each site. We observed frequent daytime sub-3 nm particle events at both sites, with a median number concentration of 2800 ± 1600 cm^{-3}, on 37 out of 46 observation days. The occurrence of the daytime events was triggered by high concentrations of H_2SO_4 and was not suppressed by coexisting large particles. The sub-3 nm particles did not grow larger than 10 nm in marine air masses, even though substantial H_2SO_4 was present at noon ($1–4 \times 10^6$ cm^{-3}). These results indicate that some condensable species, which were needed for growth in the sub-3 nm size range, were present in the continental air masses but were lacking in the marine air masses.

Nighttime events of sub-3 nm particles were observed on 6 out of 23 observation nights only in the marine air masses at Brookhaven but not in the continental air masses. During the nighttime events, sub-3 nm particles made up of 30–50% of the total nighttime particles at the coastal site. The median $N_{sub\text{-}3}$ was 1500 ± 400 cm^{-3}, and the formation rate of sub-3 nm particles was 1.0 ± 0.3 $cm^{-3}\,s^{-1}$ during the nighttime events, but these sub-3 nm particles did not grow larger. On the contrary, in the continental air masses sub-3 nm particles were significantly low (190 ± 130 cm^{-3}) during the nighttime. Our correlation analysis with $[H_2SO_4]$, various VOCs, and key trace species implies that some condensable species (other than H_2SO_4 and biogenic VOCs) were involved in the formation of sub-3 nm particles in the nighttime marine air masses, but we cannot specify these compounds at present.

Our observations did not show the persistent existence of sub-3 nm during the day and night both at Kent and Brookhaven, and rather, there were large variations in sub-3 nm particle concentrations ranging from several hundreds of particles per cubic centimeter during the nonevents to several thousands of particles per cubic centimeter during the events. This is in contrast to the observations made in the Hyytiälä boreal forest where there were consistently several thousands of particles per cubic centimeter of sub-2 nm particles regardless of event or event days continuously for 24 h [*Kulmala et al.*, 2013]. Our results also did not show

any correlations between sub-3 nm particles and the monoterpene ozonolysis product (k[MT][O_3]/CS) at Brookhaven. This is also different from the findings in the Hyytiälä boreal forest, where the diurnal variation of monoterpene oxidation products (than [H_2SO_4]) was closer to sub-3 nm particle concentrations [*Kulmala et al*., 2013; *Lehtipalo et al*., 2011]. *Kulmala et al*. [2013] suggested that for sub-2 nm particles to grow larger, several key chemical species may be involved, such as organic compounds containing nitrogen and oxygen likely formed from reactions of monoterpenes. Since the Hyytiälä forest primarily consists of pine trees, those monoterpene-derivation compounds are more abundant in Hyytiälä than in most of the other regions of the atmosphere, which can be unique to this site and may explain the persistent presence of sub-2 nm particles observed there. These results show that different nucleation processes dominate at different atmospheric conditions and perhaps these is not a universal nucleation mechanism that works for the entire atmosphere.

The nocturnal sub-3 nm particle formation in marine air mass may have important implications for the global budget of nanoparticles. When air masses are transported from the ocean to the land, sub-3 nm particles may grow more to larger particles, given higher concentrations of anthropogenic and biogenic VOCs emitted from the land surfaces. Atmospheric sub-3 nm particle measurements are still relatively scarce, in particular in the regions outside of Europe. Our observations provide important information on sub-3 nm particle occurrences in two coastal/continental locations in the United States, which will be useful for a better understanding of the atmospheric new particle formation mechanisms on the global scale. However, further long-term measurements are needed to investigate the frequency and intensity of sub-3 nm particle formation and growth in various diverse atmospheric environments.

Acknowledgments

This study was supported by DOE (subcontract number 199552) NOAA (NA08OAR4310537), NSF (Career ATM-0645567, AGS-1137821, AGS 1241498). We thank Danielle Weech and Galina Chirokova for their help in the SMPS data collection during the 2011 Aerosol Life Cycle IOP study, Katrianne Lehtipalo and Janek Uin for useful conversations on the PSM data interpretation, and two anonymous reviewers for helpful comments that improved the manuscript.

References

Andreae, M. O. (2013), The aerosol nucleation puzzle, *Science*, *339*(6122), 911–912, doi:10.1126/science.1233798.

Ball, S. M., D. R. Hanson, F. L. Eisele, and P. H. McMurry (1999), Laboratory studies of particle nucleation: Initial results for H_2SO_4, H_2O, and NH_3 vapors, *J. Geophys. Res.*, *104*, 23,709–23,718, doi:10.1029/1999JD900411.

Benson, D. R., L. H. Young, R. Kameel, and S.-H. Lee (2008), Laboratory-measured sulfuric acid and water homogeneous nucleation rates from the SO_2 + OH reaction, *Geophys. Res. Lett.*, *35*, L11801, doi:10.1029/2008GL033387.

Benson, D. R., M. E. Erupe, and S.-H. Lee (2009), Laboratory-measured H_2SO_4-H_2O-NH_3 ternary homogeneous nucleation rates: Initial observations, *Geophys. Res. Lett.*, *36*, L15818, doi:10.1029/2009GL038728.

Benson, D. R., M. Al-Refai, and S.-H. Lee (2010), Chemical ionization mass spectrometer (CIMS) for ambient measurments of ammonia, *Atmos. Meas. Tech.*, *3*, 1075–1087, doi:10.5194/amt-3-1075-2010.

Benson, D. R., H. Yu, A. Markovich, and S.-H. Lee (2011), Ternary homogeneous nucleation of H_2SO_4, NH_3, and H_2O under conditions relevant to the lower troposphere, *Atmos. Chem. Phys.*, *11*, 4755–4766, doi:10.5194/acp-11-4755-2011.

Berndt, T., O. Boge, F. Stratmann, J. Heintzenberg, and M. Kulmala (2005), Rapid formation of sulfuric acid particles at near atmospheric conditions, *Science*, *307*, 671–698, doi:10.1126/science.1104054.

Berndt, T., et al. (2010), Laboratory study on new particle formation from the reaction OH + SO_2: Influence of experimental conditions, H_2O vapour, NH_3 and the amine tert-butylamine on the overall process, *Atmos. Chem. Phys.*, *10*(15), 7101–7116, doi:10.5194/acpd-10-6447-2010.

Chen, M., et al. (2012), An acid-base chemical reaction model for nucleation rates in the polluted atmospheric boundary layer, *Proc. Natl. Acad. Sci. U. S. A.*, 18,713–18,718, doi:10.1073/pnas.1210285109.

Dal Maso, M., M. Kulmala, I. Riipinen, R. Wagner, T. Hussein, P. Aalto, and E. J. Lehtinen (2005), Formation and growth rates of fresh atmospheric aerosols: Eight years of aerosol size distribution data from SMEARII, Hyytiälä, Finland, *Boreal Environ. Res.*, *10*, 323–336.

Dawson, M. L., M. E. Varner, V. Perraud, M. J. Ezell, R. B. Gerbera, and B. J. Finlayson-Pitts (2012), New particle formation from methanesulfonic acid, amines and water: Experiment, ab initio calculations and a simplified mechanism, *Proc. Natl. Acad. Sci. U. S. A.*, 18,719–18,724, doi:10.1073/pnas.1211878109.

Donahue, N. M., J. H. Kroll, J. G. Anderson, and K. L. Demerjian (1998), Direct observation of OH production from the ozonolysis of olefins, *Geophys. Res. Lett.*, *25*(1), 59–62, doi:10.1029/97gl53560.

Donahue, N. M., E. R. Trump, J. R. Pierce, and I. Riipinen (2011), Theoretical constraints on pure vapor-pressure driven condensation of organics to ultrafine particles, *Geophys. Res. Lett.*, *38*, L16801, doi:10.1029/2011gl048115.

Draxler, R. R., and G. D. Rolph (2003), HYSPLIT (Hybrid Single-Particle Langrangian Integrated Trajectory) model access via NOAA ARL READY Website (http://www.arl.noaa.gov/HYSPLIT.php). NOAA Air Resources Laboratory, College Park, MD.

Eisele, F. L., and D. J. Tanner (1993), Measurements of gas phase concentrations of H_2SO_4 and methane sulfonic acid and estimates of H_2SO_4 production and loss in the atmosphere, *J. Geophys. Res.*, *98*, 9001–9010, doi:10.1029/93JD00031.

Eisele, F. L., E. R. Lovejoy, E. Kosciuch, K. F. Moore, R. L. Mauldin III, J. N. Smith, P. H. McMurry, and K. Iida (2006), Negative atmospheric ions and their potential role in ion-induced nucleation, *J. Geophys. Res.*, *111*, D04305, doi:10.1029/2005JD006568,

Erupe, M. E., et al. (2010), Correlation of aerosol nucleation rate with sulfuric acid and ammonia in Kent, Ohio: An atmospheric observation, *J. Geophys. Res.*, *115*, D23216, doi:10.1029/2010JD013942.

Erupe, M. E., A. A. Viggiano, and S. H. Lee (2011), The effect of trimethylamine on atmospheric nucleation involving H_2SO_4, *Atmos. Chem. Phys.*, *11*, 4767–4775, doi:10.5194/acp-11-4767-2011.

Finlayson-Pitts, B. J., and J. N. Pitts (2000), *Chemistry of the Upper and Lower Atmosphere: Theory, Experiments, and Applications*, Academic Press, San Diego, CA.

Guenther, A. B., et al. (1995), A global model of natural volatile organic compound emissions, *J. Geophys. Res.*, *100*, 8873–8892, doi:10.1029/94JD02950.

Harris, E., et al. (2013), Enhanced role of transition metal ion catalysis during in-cloud oxidation of SO_2, *Science*, *340*(6133), 727–730, doi:10.1126/science.1230911.

Hermann, M., J. Heintzenberg, A. Wiedensohler, A. Zahn, G. Heinrich, and C. A. M. Brenninkmeijer (2003), Meridional distributions of aerosol particle number concentrations in the upper troposphere and lower stratosphere obtained by Civil Aircraft for Regular Investigation of the Atmospheric Based on an Instrument Container (CARIBIC) flights, *J. Geophys. Res.*, *108*(D3), 4114, doi:10.1029/2001JD001077.

Hirsikko, A., et al. (2011), Atmospheric ions and nucleation: A review of observations, *Atmos. Chem. Phys.*, *11*(2), 767–798, doi:10.5194/acp-11-767-2011.

Hoffmann, T., J. R. Odum, F. Bowman, D. Collins, D. Klockow, R. C. Flagan, and J. H. Seinfeld (1997), Formation of organic aerosols from the oxidation of biogenic hydrocarbons, *J. Atmos. Chem.*, *26*(2), 189–222, doi:10.1023/a:1005734301837.

Jiang, J., M. Chen, C. Kuang, M. Attoui, and P. H. McMurry (2011a), Electrical mobility spectrometer using a diethylene glycol condensation particle counter for measurement of aerosol size distributions down to 1 nm, *Aerosol Sci. Technol.*, *45*(4), 510–521, doi:10.1080/02786826.2010.547538.

Jiang, J., J. Zhao, M. Chen, F. L. Eisele, J. Scheckman, B. J. Williams, C. Kuang, and P. H. McMurry (2011b), First measurements of neutral atmospheric cluster and 1-2 nm particle number size distributions during nucleation events, *Aerosol Sci. Technol.*, *45*(4), II–V, doi:10.1080/02786826.2010.546817.

Jokinen, T., M. Sipilä, H. Junninen, M. Ehn, G. Lönn, J. Hakala, T. Petäjä, R. L. Mauldin III, M. Kulmala, and D. R. Worsnop (2012), Atmospheric sulphuric acid and neutral cluster measurements using CI-APi-TOF, *Atmos. Chem. Phys.*, *12*(9), 4117–4125, doi:10.5194/acp-12-4117-2012.

Junninen, H., et al. (2008), Observations on night time growth of atmospheric clusters, *Tellus Ser. B*, *60B*, 365–371, doi:10.1111/j.1600-0889.2008.00356.x.

Junninen, H., et al. (2010), A high-resolution mass spectrometer to measure atmospheric ion composition, *Atmos. Meas. Tech.*, *3*, 1039–1053, doi:10.5194/amt-3-1039-2010.

Kanawade, V. P., A. B. Guenther, B. T. Jobson, M. E. Erupe, S. N. Pressely, S. N. Tripathi, and S.-H. Lee (2011), Isoprene suppression of new particle formation in a mixed decideous forest, *Atmos. Chem. Phys.*, *11*, 6013–6027, doi:10.5194/acp-11-6013-2011.

Kanawade, V., D. R. Benson, and S.-H. Lee (2012), Statistical analysis of 4 year measurements of aerosol sizes in a semi-rural U.S. continental environment, *Atmos. Environ.*, *59*, 30–38, doi:10.1016/j.atmosenv.2012.05.047.

Kirkby, J., et al. (2011), Role of sulphuric acid, ammonia and galactic cosmic rays in atmospheric aerosol nucleation, *Nature*, *476*(7361), 429–433, doi:10.1038/nature10343.

Korhonen, P., M. Kulmala, A. Laaksonen, Y. Viisanen, R. McGraw, and J. H. Seinfeld (1999), Ternary nucleation of H_2SO_4, NH_3, and H_2O in the atmosphere, *J. Geophys. Res.*, *104*, 26,349–26,353, doi:10.1029/1999JD900784.

Kulmala, M., M. Dal Maso, J. M. Makela, L. Pirjola, M. Vakeva, P. Aalto, P. Miikkulainen, K. Hameri, and C. D. O'Dowd (2001), On the formation, growth, and composition of nucleation mode particles, *Tellus*, *53B*, 479–490, doi:10.1034/j.1600-0889.2001.530411.x.

Kulmala, M., V. M. Kerminen, T. Anntila, A. Laaksonen, and C. D. O'Dowd (2004a), Organic aerosol formation via sulfate cluster activation, *J. Geophys. Res.*, *109*, D04205, doi:10.1029/2003JD003961.

Kulmala, M., L. Laakso, K. E. J. Lehtinen, I. Riipinen, M. Dal Maso, A. Lauria, V.-M. Kerminen, W. Birmili, and P. H. McMurry (2004b), Formation and growth rates of ultrafine atmosphere particles: A review of observations, *J. Aerosol Sci.*, *35*, 143–176, doi:10.1016/j.jaerosci.2003.10.003.

Kulmala, M., et al. (2007), Toward direct measurement of atmospheric nucleation, *Science*, *318*, 89–92, doi:10.1126/science.1144124.

Kulmala, M., et al. (2013), Direct observations of atmospheric aerosol nucleation, *Science*, *339*(6122), 943–946, doi:10.1126/science.1227385.

Laakso, L., T. Petaja, K. E. J. Lehtinen, M. Kulmala, J. Paatero, U. Horrack, H. Tammet, and J. Joutsensaari (2004), Ion production rate in a boreal forest based on ion, particle, and radiation measurements, *Atmos. Chem. Phys.*, *4*, 1933–1943, doi:10.5194/acp-4-1933-2004.

Lee, S.-H., J. M. Reeves, J. C. Wilson, D. E. Hunton, A. A. Viggiano, T. M. Miller, J. O. Ballenthin, and L. R. Lait (2003), Particle formation by ion nucleation in the upper troposphere and lower stratosphere, *Science*, *301*, 1886–1889, doi:10.1126/science.1087236.

Lee, S.-H., L. H. Young, D. R. Benson, M. Kulmala, H. Junninen, T. Suni, T. Campos, D. C. Rogers, and J. Jensen (2008), Observations of nighttime new particle formation in the troposphere, *J. Geophys. Res.*, *113*, D10210, doi:10.1029/2007JD009351.

Lehtipalo, K., M. Sipilä, I. Riipinen, T. Nieminen, and M. Kulmala (2009), Analysis of atmospheric neutral and charged molecular clusters in boreal forest using pulse-height CPC, *Atmos. Chem. Phys.*, *9*, 4177–4184.

Lehtipalo, K., M. Kulmala, M. Sipilä, T. Petäjä, M. Vana, D. Ceburnis, R. Dupuy, and C. O'Dowd (2010), Nanoparticles in boreal forest and coastal environment: A comparison of observations and implications of the nucleation mechanism, *Atmos. Chem. Phys.*, *10*, 7009–7016, doi:10.5194/acp-10-7009-2010.

Lehtipalo, K., M. Sipila, H. Junninen, M. Ehn, T. Berndt, M. K. Kajos, D. R. Worsnop, T. Petaja, and M. Kulmala (2011), Observations of Nano-CN in the Nocturnal Boreal Forest, *Aerosol Sci. Technol.*, *45*(4), 499–509, doi:10.1080/02786826.2010.547537.

Lovejoy, E. R., J. Curtius, and K. D. Froyd (2004), Atmospheric ion-induced nucleation of sulfuric acid and water, *J. Geophys. Res.*, *109*, D08204, doi:10.1029/2003JD004460.

Mauldin III, R. L., T. Berndt, M. Sipila, P. Paasonen, T. Petaja, S. Kim, T. Kurten, F. Stratmann, V. M. Kerminen, and M. Kulmala (2012), A new atmospherically relevant oxidant of sulphur dioxide, *Nature*, *488*(7410), 193–196, doi:10.1038/nature11278.

Merikanto, J., D. V. Spracklen, G. W. Mann, S. J. Pickering, and K. S. Carslaw (2009), Impact of nucleation on global CCN, *Atmos. Chem. Phys.*, *9*, 8601–8616, doi:10.5194/acp-9-8601-2009.

Metzger, A., et al. (2010), Evidence for the role of organics in aerosol particle formation under atmospheric conditions, *Proc. Natl. Acad. Sci. U. S. A.*, *107*(15), 6646–6651, doi:10.1073/pnas.0911330107.

Nieminen, T., K. E. J. Lehtinen, and M. Kulmala (2010), Sub-10 nm particle growth by vapor condensation—Effects of vapor molecule size and particle thermal speed, *Atmos. Chem. Phys.*, *10*(20), 9773–9779, doi:10.5194/acp-10-9773-2010.

Nilsson, E. D., J. Paatero, and M. Boy (2001), Effects of air masses and synoptic weather on aersol formation in the continental boundary layer, *Tellus Ser. B*, *53*(4), 462–478, doi:10.1034/j.1600-0889.2001.530410.x.

O'Dowd, C. D., P. Aalto, K. Hameri, M. Kulmala, and M. R. Hoffmann (2002a), Atmospheric particles from organic vapors, *Nature*, *416*, 497–498, doi:10.1038/416497a.

O'Dowd, C. D., J. L. Jimenez, R. Bahreini, R. C. Flagan, J. H. Seinfeld, K. Mammary, L. Pirjola, M. Kulmala, S. G. Jennings, and M. R. Hoffmann (2002b), Marine aerosol formation from biogenic iodine emisssions, *Nature*, *417*, 632–636, doi:10.1038/nature00775.

Ortega, I. K., T. Suni, T. Gronholm, M. Boy, H. Hakola, H. Hellen, T. Valmari, H. Arvela, H. Vehkamaki, and M. Kulmala (2009), Is eucalyptol the cause of nocturnal events observed in Australia?, *Boreal Environ. Res.*, *14*(4), 606–615.

Ortega, I. K., et al. (2012), New insights into nocturnal nucleation, *Atmos. Chem. Phys.*, *12*(9), 4297–4312, doi:10.5194/acp-12-4297-2012.

Paulson, S. E., A. D. Sen, P. Liu, J. D. Fenske, and M. J. Fox (1997), Evidence for the formation of OH radicals from the reaction of O_3 with alkenes in the gas phase, *Geophys. Res. Lett.*, *24*, 3193–3196, doi:10.1029/97GL03163.

Paulson, S. E., M. Y. Chung, and A. S. Hasson (1999), OH radical formation from the gas-phase reaction of ozone with terminal alkenes and the relationship between structure and mechanism, *J. Phys. Chem. A*, *103*(41), 8125–8138, doi:10.1021/jp991995e.

Riccobono, F., et al. (2012), Contribution of sulfuric acid and oxidized organic compounds to particle formation and growth, *Atmos. Chem. Phys.*, *12*, 9427–9439, doi:10.5194/acp-12-9427-2012.

Riipinen, I., T. Yli-Juuti, J. R. Pierce, T. Petaja, D. R. Worsnop, M. Kulmala, and N. M. Donahue (2012), The contribution of organics to atmospheric nanoparticle growth, *Nat. Geosci.*, *5*(7), 453–458, doi:10.1038/ngeo1499.

Russell, L. M., A. A. Mensah, E. V. Fischer, B. C. Sive, R. K. Varner, W. C. Keene, J. Stutz, and A. A. P. Pszenny (2007), Nanoparticle growth following photochemical α-pinene and β-pinene oxidation at Appledore Island during International Consortium for Research on Transport and Transformation/Chemistry of Halogens at the Isles of Shoals 2004, *J. Geophys. Res.*, *112*, D10S21, doi:10.1029/2006jd007736.

Sedlacek, A., E. R. Lewis, L. Kleinman, J. Z. Xu, and Q. Zhang (2012), Determination of and evidence for non-core-shell structure of particles containing black carbon using the single particle soot photometer (SP2), *Geophys. Res. Lett.*, *39*, L06802, doi:10.1029/2012GL050905.

Seinfeld, J. H., and S. N. Pandis (2006), *Atmospheric Chemistry and Physics: From Air Pollution to Climate Change*, 2nd ed., John Wiley, New York.

Sipila, M., K. Lehtipalo, M. Attoui, K. Neitola, T. Petaja, P. P. Aalto, C. D. O'Dowd, and M. Kulmala (2009), Laboratory verification of PH-CPC's ability to monitor atmospheric sub-3 nm clusters, *Aerosol Sci. Technol.*, *43*(2), 126–135, doi:10.1080/02786820802506227.

Sipila, M., et al. (2010), The role of sulfuric acid in atmospheric nucleation, *Science*, *327*, 1243–1246, doi:10.1126/science.1180315.

Sogacheva, L., L. Saukkonen, E. D. Nilsson, M. Dal Maso, D. M. Schultz, G. De Leeuw, and M. Kulmala (2008), New aerosol particle formation in different synoptic situations at Hyytiälä, Southern Finland, *Tellus Ser. B*, *60*(4), 485–494, doi:10.1111/j.1600-0889.2008.00364.x.

Suni, T., et al. (2008), Formation and characteristics of ions and charged aerosol particles in a native Australian Eucalypt forest, *Atmos. Chem. Phys.*, *8*(1), 129–139, doi:10.5194/acp-8-129-2008.

Svenningsson, B., et al. (2008), Aerosol particle formation events and analysis of high growth rates observed above a subarctic wetland-forest mosaic, *Tellus*, *60*(B), 353–365, doi:10.1111/j.1600-0889.2008.00351.x.

Tammet, H. (2011), Symmetric inclined grid mobility analyzer for the measurement of charged clusters and fine nanoparticles in atmospheric air, *Aerosol Sci. Technol.*, *45*, 468–479, doi:10.1080/02786826.2010.546818.

Vana, M., M. Ehn, T. Petäjä, H. Vuollekoski, P. Aalto, G. de Leeuw, D. Ceburnis, C. D. O'Dowd, and M. Kulmala (2008), Characteristic features of air ions at Mace Head on the west coast of Ireland, *Atmos. Res.*, *90*(2-4), 278–286, doi:10.1016/j.atmosres.2008.04.007.

Vanhanen, J., J. Mikkila, K. Lehtipalo, M. Sipila, H. E. Manninen, E. Siivola, T. Petaja, and M. Kulmala (2011), Particle size magnifier for nano-CN detection, *Aerosol Sci. Technol.*, *45*(4), 533–542, doi:10.1080/02786826.2010.547889.

Vehkamäki, H., M. Kulmala, I. Napari, E. J. Lehtinen, C. Timmreck, M. Noppel, and A. Laaksonen (2002), An improved parameterization for sulfuric acid-water nucleation rates for tropospheric and stratospheric conditions, *J. Geophys. Res.*, *107*(D22), 4622, doi:10.1029/2002JD002184.

Verheggen, B., and M. Mozurkewich (2006), An inverse modeling procedure to determine particle growth and nucleation rates from measured aerosol size distributions, *Atmos. Chem. Phys.*, *6*, 2927–2942, doi:10.5194/acp-6-2927-2006.

Wang, J., and A. S. Wexler (2013), Adsorption of organic molecules may explain growth of newly nucleated clusters and new particle formation, *Geophys. Res. Lett.*, *40*, 2834–2838, doi:10.1002/grl.50455.

Weber, R. J., J. J. Marti, P. H. McMurry, F. L. Eisele, D. Tanner, and A. Jefferson (1996), Measured atmospheric new particle formation rates: Implications for nucleation mechanisms, *Chem. Eng. Commun.*, *151*, 53–64, doi:10.1029/96JD03656.

Wiedensohler, A., et al. (1997), Night-time formation and occurence of new particles associated with orographic clouds, *Atmos. Environ.*, *31*(16), 2545–2559, doi:10.1016/S1352-2310(96)00299-3.

Wyslouzil, B. E., J. H. Seinfeld, R. C. Flagan, and K. Okuyama (1991), Binary nucleation in acid-water systems. II Sulphuric acid-water and a comparison with methanesulphonic acid-water, *J. Chem. Phys.*, *94*, 6842–6850, doi:10.1063/1.460262.

Young, L. H., D. R. Benson, F. Rifkha, J. R. Pierce, H. Junninen, M. Kulmala, and S.-H. Lee (2008), Laboratory studies of sulfuric acid and water binary homogeneous nucleation: Evaluation of laboratory setup and preliminary results, *Atmos. Chem. Phys.*, *8*, 1–20, doi:10.5194/acp-8-4997-2008.

Yu, H., and S.-H. Lee (2012), A chemical ionization mass spectrometer for the detection of atmospheric amines, *Environ. Chem.*, *9*, 190–201, doi:10.1071/EN12020.

Yu, H., R. McGraw, and S.-H. Lee (2012), Effects of amines on formation of sub-3 nm particles and their subsequent growth, *Geophys. Res. Lett.*, *39*, L02807, doi:10.1029/2011GL050099.

Yu, F., R. P. Turco, B. Karcher, and F. P. Schroder (1998), On the mechanisms controlling the formation and properties of volatile particles in aircraft wakes, *Geophys. Res. Lett.*, *25*, 3839–3842, doi:10.1029/1999GL900324.

Yu, F., Z. Wang, G. Luo, and R. Turco (2008), Ion-mediated nucleation as an important global source of tropospheric aerosols, *Atmos. Chem. Phys.*, *8*, 2537–2554, doi:10.5194/acp-8-2537-2008.

Zhang, R. Y., I. Suh, J. Zhao, D. Zhang, E. C. Fortner, X. X. Tie, L. T. Molina, and M. J. Molina (2004), Atmospheric new particle formation enhanced by organic acids, *Science*, *304*, 1487–1490, doi:10.1126/science.1095139.

Zhang, R., A. Khalizov, L. Wang, M. Hu, and W. Xu (2012), Nucleation and growth of nanoparticles in the atmosphere, *Chem. Rev.*, *112*, 957–2011, doi:10.1021/cr2001756.

Zhao, J., F. L. Eisele, M. Titcombe, C. Kuang, and P. H. McMurry (2010), Chemical ionization mass spectrometric measurements of atmospheric neutral clusters using the cluster-CIMS, *J. Geophys. Res.*, *115*, D08205, doi:10.1029/2009JD012606.

Zhao, J., J. N. Smith, F. L. Eisele, M. Chen, C. Kuang, and P. H. McMurry (2011), Observation of neutral sulfuric acid-amine containing clusters in laboratory and ambient measurements, *Atmos. Chem. Phys.*, *11*, 10,823–10,836, doi:10.5194/acp-11-10823-2011.

Zollner, J. H., W. A. Glasoe, B. Panta, K. K. Carlson, P. H. McMurry, and D. R. Hanson (2012), Sulfuric acid nucleation: Power dependencies, variation with relative humidity, and effect of bases, *Atmos. Chem. Phys.*, *12*, 4399–4411, doi:10.5194/acp-12-4399-2012.